Rice University

Distributed Full-duplex via Wireless Side Channels: Bounds and Protocols

by

Jingwen Bai

A Thesis Submitted
in Partial Fulfillment of the
Requirements for the Degree

Master of Science

Approved, Thesis Committee:

_____

Dr. Ashutosh Sabharwal, *Chair*
Professor of Electrical and Computer Engineering, Rice University

_____

Dr. Behnaam Aazhang
J.S. Abercrombie Professor of Electrical and Computer Engineering, Rice University

_____

Dr. Edward Knightly
Professor of Electrical and Computer Engineering, Rice University

Houston, Texas
March 2013

Rice University

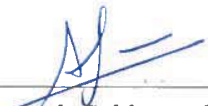# Distributed Full-duplex via Wireless Side Channels: Bounds and Protocols
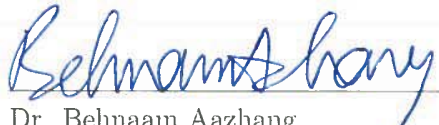
by

Jingwen Bai

A Thesis Submitted
in Partial Fulfillment of the
Requirements for the Degree

Master of Science

Approved, Thesis Committee:

Dr. Ashutosh Sabharwal, *Chair*
Professor of Electrical and Computer Engineering, Rice University

Dr. Behnaam Aazhang
J.S. Abercrombie Professor of Electrical and Computer Engineering, Rice University

Dr. Edward Knightly
Professor of Electrical and Computer Engineering, Rice University

Houston, Texas
March 2013

Abstract

Distributed Full-duplex via Wireless Side Channels: Bounds and Protocols

by

Jingwen Bai

In this thesis, we study a three-node full-duplex network, where the infrastructure node has simultaneous up- and downlink communication in the same frequency band with two half-duplex nodes. In addition to self-interference at the full-duplex infrastructure node, the three-node network has to contend with the inter-node interference between the two half-duplex nodes. The two forms of interferences differ in one important aspect that the self-interference is known at the interfered receiver. Therefore, we propose to leverage a wireless side-channel to manage the inter-node interference. We characterize the impact of inter-node interference on the network achievable rate region with and without a side-channel between the nodes. We present four distributed full-duplex inter-node interference cancellation schemes, which leverage the device-to-device wireless side-channel for improved interference cancellation. Of the four, bin-and-cancel is asymptotically optimal in high signal-to-noise ratio limit which uses Han-Kobayashi common-private message splitting and achieves within 1 bit/s/Hz of the capacity region for all values of channel parameters. The other three schemes are simpler compared to bin-and-cancel but achieve the near-optimal performance only in certain regimes of channel values. Asymptotic multiplexing gains of all proposed schemes are derived

to show analytically that leveraging the side channel can be highly beneficial in increasing the multiplexing gain of the system exactly in those regimes where inter-node interference has the highest impact.

Acknowledgements

First of all, I would like to express my sincere gratitude to my advisor, Ashutosh Sabharwal, for guiding me and making this thesis into reality. In addition, I'm very grateful to my colleagues for their support and feedback along the whole process.

Finally, I would like to extend my deepest gratitude to my parents, Limin Bai and Yanhong Guo, for their endless love and encouragement. Without their support, I would not have a chance to be in U.S. for graduate study and I would never find the courage to overcome all the difficulties during the work.

Contents

List of Figures

List of Tables

Introduction

1.1 Three-node Full-duplex Network

Full-duplex wireless communication has recently been shown [5, 8, 4, 9, 10, 17, 14, 13, 16] to promise higher spectral efficiency than the half-duplex paradigm for short to medium range bi-directional communications when both mobile and infrastructure nodes are full-duplex, in which the transmission and reception are done in the same time and frequency signaling dimensions. Most of the work till date on full-duplex communications has focused on the bidirectional communications between two nodes. An alternate use of full-duplex capability is a three-node network [14] shown in Figure 1.1, where a full-duplex infrastructure node can communicate with two half-duplex mobiles simultaneously to support one uplink and one downlink flow. Since there is more flexibility in the design of infrastructure nodes, it is possible to suppress self-interference much more in infrastructure nodes than space-constrained mobile devices. In fact, well designed passive suppression techniques [13] can extend ranges significantly in outdoor environments. Thus, we envision that the first adoption of full-duplex will be at the infrastructure nodes, such as femto base stations and WiFi access points, while space-constrained mobile devices will continue to be half-duplex.

As shown in Fig. 1.1, the mobile node 1 (M1) is uploading data to the full-duplex base station while mobile node 2 (M2) is downloading data from base station simultaneously in the same band. Since wireless communication is broadcast by nature, the three-node network shown in Figure 1.1 has to deal with two forms of interferences: self-interference at the full-duplex infrastructure node, and inter-node interference (INI) from uplink Mobile M1 to downlink Mobile M2.
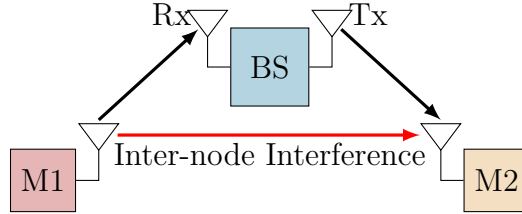
Figure 1.1: Three-node full-duplex network: inter-node interference becomes an important factor when the infrastructure node communicates with uplink and downlink mobile nodes simultaneously.

1.2   Distributed-full-duplex

The two forms of interferences in the three-node network differ in one important aspect that the self-interference is known at the interfered receiver, since the transmitter and receiver are co-located at BS while the inter-node interference is unknown to the unintended receiver of M2 because the transmitter of M1 and interfered receiver of M2 is distributed.

In this thesis, we study how a wireless side-channel between Nodes M1 and M2 can be leveraged to manage INI. Conceptually, one can model the co-location of transmitter and receiver on a full-duplex node as an infinite capacity side channel. Thus, our use of a wireless side channel between M1 and M2 mimics the inherent full-duplex side channel but has finite bandwidth and signal-to-noise ratio (SNR) like

any practical wireless channel. The wireless side-channel model is inspired by the fact that most smartphones support simultaneous use of multiple standards, and can thus access multiple orthogonal spectral bands. For example, the whole network could be on a cellular band while the M1-M2 wireless side channel could be in the unlicensed ISM band.

We label the protocols for communication in side-channel assisted three-node network as *distributed full-duplex*. In this thesis, we assume that the self-interference has been suppressed to the noise floor and hence focus on INI.

Note that although we propose distributed full-duplex via wireless side channels for interference canellation in the three-node full-duplex network, the three-node network topology is just a motivation example. Our proposed distributed full-duplex is a more general concept: by leveraging the wireless side channel, we can enable simultaneously transmission and reception in the same frequency band when the transmitter and interfered receiver are distributed but within communication range, by analogy to the self-interference cancellation mechanism used in bidirectional full-duplex (two-way) communication where the transmitter and interfered receiver are co-located in the same node.

1.3   Main Contributions

We make the following main technical contributions. First of all, we investigate the baseline performance of the three-node network without any side channels. We model the three-node network as a cognitive Z-channel to derive the inner and outer bound on the capacity region. Asymptotic sum-capacity is established in the high SNR limit. As expected, a multiplexing gain of two is achievable in the very weak and very strong interference regimes, but the INI causes the multiplexing gain to reduce significantly in all other regimes.

Secondly, we propose four distributed full-duplex inter-node interference cancelation schemes by leveraging a device-to-device wireless side channel for improved interference cancellation. The four schemes are labeled bin-and-cancel (BC), compress-and-cancel (CC), decode-and-cancel (DC) and estimate-and-cancel (EC). All schemes rely on the side channel, to send information about the INI from Node M1 to Node M2. Since the side-channel is an orthogonal channel, Node M1 uses the side channel signal as side information while decoding its signal of interest from BS. As the names suggest, all four schemes encode the M1 signal on the side channel in different ways. Of the four, bin-and-cancel is the most sophisticated, uses Han-Kobayashi style common-private message splitting and can achieve within 1 bit/s/Hz of the capacity region for *all* values of channel parameters. The other three schemes are simpler compared to bin-and-cancel but achieve the near-optimal (finite approximation) performance only in certain regimes of channel values; we derive exact regions of approximate optimality for decode- and estimate-and-cancel.

Second, we derive the asymptotic multiplexing gains of bin-, compress-, decode-, estimate-and-cancel schemes. We show analytically that the side information can be highly beneficial in increasing the multiplexing gain of the system exactly in those regimes where INI has the highest impact. We provide exact characterization of how the extra bandwidth of the side channel can be leveraged to achieve the multiplexing gains. As expected, the multiplexing gain scales with the bandwidth of the side channel and can reach the maximum value which no longer depends on additional bandwidth of the side channel. Finally, we show numerically that significant multiplexing gains are available for finite SNRs of practical interest, and thus our analysis make a case for using wireless spectrum in a more flexible manner (e.g unlicensed bands in licensed spectrum).

1.4 Organization of the Thesis

The rest of the thesis is organized as follows. Chapter 2 presents system model and the impact of inter-node interference in the three-node full-duplex network without a side channel. In Chapter 3, we propose four distributed full-duplex interference cancellation schemes for side-channel assisted three-node network and obtain information theoretical results on their achievable rates. Chapter 4 gives the bounds on the capacity region of the side-channel assisted three-node network. Chapter 5 characterizes the performance of different schemes, including both finite SNR results as well as high SNR capacity approximatons. Chapter 6 opens up the discussion with respect to spectral efficiency of different systems with/without using the side channel. Chapter 7 concludes the thesis.

No Side Channel Bounds on Gaussian Three-node Full-duplex Channel

2.1 System Model

In this section, we will describe the system model to be used for the rest of the thesis. We assume the self-interference at the full-duplex base station is below the noise floor, the resulting network is modeled as a as shown in Fig. 2.1. We have per-node power constraint for each transmitter, let P_1, P_2 denote the total power constraint for the transmitter of BS and Node M1, respectively. And let W_m, W_s denote the bandwidth for the main channel and side channel, respectively. Parameter $W = \frac{W_s}{W_m}$ represents the bandwidth ratio of the side channel to that of the main channel, where $W \in [0, W_{\max}]$.

The following equations capture the input-output relationship between transmitted and received signals:

$$Y_1 = \gamma_1 X_1 + \gamma_{21}^m X_2 + Z_1$$

$$Y_2 = \gamma_2 X_2 + Z_2$$

$$Y_3 = \gamma_{21}^s X_3 + Z_3,$$
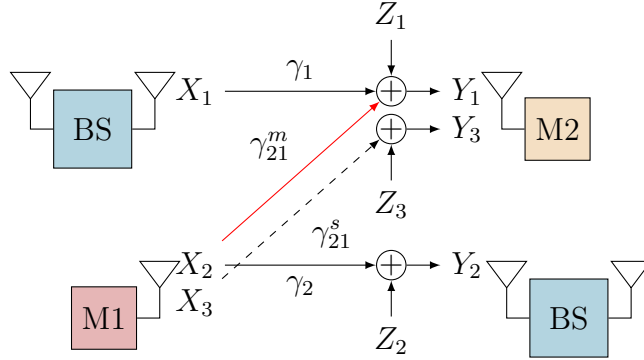
Figure 2.1: System model: Z-channel with side channel.

where for $i = 1, 2, 3$, X_i is the codeword with input power constraint $\mathbb{E}(|X_1|^2) \leq P_1$, $\mathbb{E}(|X_2 + X_3|^2) \leq P_2$. Let Z_i be i.i.d. white Gaussian noise with zero mean and variance of σ^2. The coefficients γ_1, γ_2 are the channel gains of the direct link from the transmitters to their intended receivers, γ_{21}^m is the channel gain of the interference link from M1 to M2, and γ_{21}^s be the channel gain of the side channel from M1 to M2. To simplify the notation, let $\text{SNR}_1 = \frac{|\gamma_1|^2 P_1}{\sigma^2}, \text{SNR}_2 = \frac{|\gamma_2|^2 P_2}{\sigma^2}, \text{INR} = \frac{|\gamma_{21}^m|^2 P_2}{\sigma^2}$ and $\text{SNR}_{\text{side}} = \frac{|\gamma_{21}^s|^2 P_2}{\sigma^2}$.

There are two independent uniformly distributed index sets $s_i \in [1 : 2^{nR_i}], i = 1, 2$, which belong to base station and uplink M1, respectively. The encoding function $f_i : [1 : 2^{nR_i}] \rightarrow C_k, k = 1, 2, 3$ yields codewords $X_k{}^n(s_i)$ for block length n. The codewords satisfy

$$\frac{1}{n}\sum_{i=1}^{n} E(|X_{1i}|^2) \leq P_1, \frac{1}{n}\sum_{i=1}^{n} E(|X_{2i} + X_{3i}|^2) \leq P_2.$$

Receiver of downlink M2 uses decoding functions $g_1 : C_k \rightarrow \in [1 : 2^{nR_1}], k = 1, 3$ to map the received sequence y_k^n into a message $\hat{s}_1$. And receiver of base station uses a decoding function $g_2 : C_2 \rightarrow \in [1 : 2^{nR_2}]$ to map the received sequence y_2^n into a

message $\hat{s}_2$.

$$\lambda_1{}^n = \frac{1}{S_1 S_2} \sum_{s_1, s_2,} \mathrm{Prob}\left(g_1(Y_1{}^n, Y_3{}^n) \neq s_1 | S_1 = s_1\right),$$

$$\lambda_2{}^n = \frac{1}{S_1 S_2} \sum_{s_1, s_2,} \mathrm{Prob}\left(g_2(Y_2{}^n)) \neq s_2 | S_2 = s_2\right), \tag{2.1}$$

$$\lambda^n = \max\left(\lambda_i{}^n\right), i = 1, 2.$$

A rate pair (R_1, R_2) is said to be achievable if there exists a sequence of $\left(2^{nR_1}, 2^{nR_2}, n\right)$ codes such that the maximal probability of error λ^n goes to 0 as n goes to ∞. The capacity region is the closure of the set of all achievable rate pairs.

2.2   No-side-channel Inner Bound

To start with, we study the inner bound and outer bound on the capacity region of the Gaussian three-node full-duplex channel to understand the impact of INI. From Fig. 2.1, let $Y_3 = 0$ and $W = 0$, thus we can obtain the channel model without side channel.

We notice that one of the transmitter and receiver pairs in Fig. 2.1 is co-located in the base station, thus causal information of transmitter M1 is available at the transmitter of base station. This model is similar to the causal cognitive Z-interference channel [19]. In the cognitive Z-interference channel the transmitter of the secondary user has access to causal knowledge of the primary user, and there is only one interference link from the primary transmitter to the secondary receiver. Hence the three-node full-duplex channel can be modeled as cognitive Z-interference channel.

When we do not use the causal information at BS, the resulting channel is classic Z-channel. The rate region of classic Z-channel is the existing capacity inner bound of cognitive Z-interference channel. The capacity region of classic Z-channel is established in the strong and very strong interference regimes [3, 18] and Han-Kobayashi

strategies [15] yields the best achievable rate region in the weak interference regime. The sum-rate of classic Z-channel can be achieved by treating interference as noise in the weak regime and joint decoding in the strong interference regime.

In the cognitive Z-interference channel, we assume that at time i, the encoder of base station will have access to the information sequence sent by M1 up to time $i-1$. The state-of-art approaches based on block markov codes [19, 2] do not seem to help enhance the achievable rate region over the classic Z-channel (as far as is known to the author). This might result from the two main reasons below. First of all, in the two-user interference channel as described in [19], the causal information may help increase the achievable rate region, since more information can be delivered through the cross link from secondary user to the primary user by cooperative transmission. While in our case, one of the cross link has already been removed. The uplink from M1 to base station is interference-free, therefore uplink rate can not benefit from the causal information available at base station. Secondly, at time i, the way that the transmitter of base station can obtain the causal message of M1 is by decoding the message through the direct link between M1 and base station before time i. While using block markov codes, the decoding strategies at the receiver involve delay, whether using backward decoding, successive decoding or sliding window decoding. Hence we can not take advantage of the decoding schemes for block markov codes. In [19, 2], the secondary user has access to the causal message of the primary user through another link which has a different channel gain from the direct link. As shown in [19], only when the channel gain of the other link is larger than that of the direct link can the achievable rate region be increased. Otherwise, there would be no improvement on the achievable rate region. Unlike system model in [19], in our case, the channel link from which base station can acquire the causal information of M1 is the same direct link. Hence we may conjecture that this causal information will not

help improve the achievable sum-rate over Z-channel.

The inner bound on the capacity region for the Gaussian three-node full-duplex channel is given as follows.

Proposition 1. *[Weak Interference Regime [15]] When the channel parameters satisfy* $\text{INR} \leq \text{SNR}_2$,

$$
\begin{aligned}
R_1 &\leq C\left(\frac{\text{SNR}_1}{1 + \beta\text{INR}}\right) \\
R_2 &\leq \min\left\{C\left(\text{SNR}_2\right), C\left(\beta\text{SNR}_2\right) + C\left(\frac{\bar{\beta}\text{INR}}{1 + \beta\text{INR}}\right)\right\} \\
R_1 + R_2 &\leq C\left(\text{SNR}_2\right) + C\left(\frac{\text{SNR}_1}{1 + \text{INR}}\right),
\end{aligned}
\tag{2.2}
$$

where $\beta \in [0, 1], \bar{\beta} + \beta = 1,$ *and* $C(X) = W_m\log\left(1 + X\right).$

[Strong Interference Regime [18]] When the channel parameters satisfy $\text{SNR}_2 \leq \text{INR} \leq \text{SNR}_2\left(1 + \text{SNR}_1\right),$

$$
\begin{aligned}
R_1 &\leq C\left(\text{SNR}_1\right) \\
R_2 &\leq C\left(\text{SNR}_2\right) \\
R_1 + R_2 &\leq C\left(\text{SNR}_1 + \text{INR}\right).
\end{aligned}
\tag{2.3}
$$

[Very Strong Interference Regime [3]] When the channel parameters satisfy $\text{INR} \geq \text{SNR}_2\left(1 + \text{SNR}_1\right),$

$$
\begin{aligned}
R_1 &\leq C\left(\text{SNR}_1\right) \\
R_2 &\leq C\left(\text{SNR}_2\right).
\end{aligned}
\tag{2.4}
$$

2.3   No-side-channel Outer Bound

We also give the outer bound on the capacity of the Gaussian three-node full-duplex channel. If the base station knows the information of M1 non-causally, which means the BS not only knows the message of M1 in previous transmission blocks, but also the message of M1 for future transmission, then the results are trivial. Because by applying dirty paper coding [6], base station can encode its own message while treating M1's signal as known interference, thus the impact of the inter-node interference can be eliminated at receiver M2.

Since the base station only has causal knowledge of M1, we can derive the following theorem according to [11].

Theorem 1. *In the weak interference regime defined by* $\mathrm{INR} \leq \mathrm{SNR}_2$, *the capacity outer bound for the Gaussian three-node full-duplex channel is given by:*

$$
\begin{aligned}
R_1 &\leq C\left(\mathrm{SNR}_1\right) \\
R_2 &\leq C\left(\mathrm{SNR}_2\right) \\
R_1 + R_2 &\leq C(\alpha \mathrm{SNR}_2) + C\left(\frac{\bar{\alpha}\mathrm{INR} + \mathrm{SNR}_1 + 2\sqrt{\bar{\alpha}\mathrm{SNR}_1\mathrm{INR}}}{1 + \alpha\mathrm{INR}}\right),
\end{aligned}
\tag{2.5}
$$

where $\alpha \in [0,1], \alpha + \bar{\alpha} = 1$.

In the strong interference regime defined by $\mathrm{SNR}_2 \leq \mathrm{INR} \leq \mathrm{INR}^*$, *where*

$$
\mathrm{INR}^* = \mathrm{SNR}_2(1 + \mathrm{SNR}_1) + 2\mathrm{SNR}_1 - 2\sqrt{\mathrm{SNR}_1(\mathrm{SNR}_1 + \mathrm{SNR}_2 + \mathrm{SNR}_1\mathrm{SNR}_2)}, \tag{2.6}
$$

the capacity outer bound is given by

$$R_1 \leq C\left(\text{SNR}_1\right)$$

$$R_2 \leq C\left(\text{SNR}_2\right) \tag{2.7}$$

$$R_+ R_2 \leq C\left(\text{SNR}_1 + \text{INR} + 2\sqrt{\text{SNR}_1 \text{INR}}\right).$$

In the very strong interference regime defined by $\text{INR} \geq \text{INR}^*$,

$$R_1 \leq C\left(\text{SNR}_1\right)$$

$$R_2 \leq C\left(\text{SNR}_2\right). \tag{2.8}$$

Proof. The bounds on R_1 and R_2 come from the point-to-point capacity of AWGN channel. Messages $S1$ and S_2 are chosen uniformly and independently at random. X_{1i} is a function of (S_1, Y_2^{i-1}), and we define $U_i = (S_1, Y_2^{i-1}, X_1^{i-1})$ for $i \in [1, n]$. Thus by Fano's inequality,

$$
\begin{aligned}
nR_1 &\leq\ I(S_1; Y_1{}^n) + n\epsilon_1 & (2.9) \\
&=\ \sum_{i=1}^{n} I(S_1; Y_{1i}|Y_1^{i-1}) + n\epsilon_1 & (2.10) \\
&\leq\ \sum_{i=1}^{n} I(S_1, Y_1^{i-1}; Y_{1i}) + n\epsilon_1 & (2.11) \\
&\leq\ \sum_{i=1}^{n} I(S_1, Y_2^{i-1}, Y_1^{i-1}; Y_{1i}) + n\epsilon_1 & (2.12) \\
&=\ \sum_{i=1}^{n} I(S_1, Y_2^{i-1}, X_1^{i}, Y_1^{i-1}; Y_{1i}) + n\epsilon_1 & (2.13) \\
&=\ \sum_{i=1}^{n} I(S_1, Y_2^{i-1}, X_1^{i}; Y_{1i}) + n\epsilon_1 & (2.14) \\
&=\ \sum_{i=1}^{n} I(U_i, X_{1i}; Y_{1i}) + n\epsilon_1, & (2.15)
\end{aligned}
$$

where (4.10) and (4.12) follow because X_{1i} is a function of (S_1, Y_2^{i-1}); (4.11) follows

because $Y_1^{i-1} \to (X_1^i, Y_2^{i-1}) \to Y_{1i}$ forms a Markov chain. And for any codebook of block length n, we have

$$
\begin{align}
nR_2 &= H(S_2|S_1) \tag{2.16} \\
&= I(S_2; Y_2^{~n}|S_1) + H(S_2|Y_2^n, S_1) \tag{2.17} \\
&\leq I(S_2; Y_2^{~n}|S_1) + n\epsilon_2 \tag{2.18} \\
&= \sum_{i=1}^{n} I(S_2; Y_{2i}|Y_2^{i-1}, S_1) + n\epsilon_2 \tag{2.19} \\
&= \sum_{i=1}^{n} I(S_2, Y_{2i}|Y_2^{i-1}, S_1, X_1^i) + n\epsilon_2 \tag{2.20} \\
&\leq \sum_{i=1}^{n} I(X_{2i}, Y_{2i}|U_i, X_{1i}) + n\epsilon_2, \tag{2.21}
\end{align}
$$

where (4.15) follows from Fano's inequality; (4.17) follows because X_{1i} is a function of (S_1, Y_2^{i-1}).

Now by applying the standard time sharing argument, we can obtain

$$
R_1 + R_2 \leq I(U, X_1; Y_1) + I(X_2, Y_2|U, X_1), \tag{2.22}
$$

for product distribution $p(u)p(x_1 x_2|u)p(y_1 y_2|x_1 x_2)$.

Similarly, in the strong interference regime where $I(X_2; Y_2|X_1, U) \leq I(X_2; Y_1|X_1, U)$, the sum-capacity upper bound is given by

$$
\begin{align}
R_1 + R_2 &\leq I(U, X_1; Y_1) + I(X_2, Y_2|U, X_1) \tag{2.23} \\
&\leq I(U, X_1; Y_1) + I(X_2, Y_1|U, X_1) \tag{2.24} \\
&= I(U, X_1, X_2; Y_1) \tag{2.25}
\end{align}
$$

In the Gaussian channels, the capacity region is upper bounded by Gaussian

inputs. The auxiliary random variable U captures the correlation between the codewords X_1 and X_2. We define $\alpha = 1 - \rho^2$, where ρ is the correlation coefficient between X_1 and X_2 and $\alpha \in [0, 1]$. Hence the capacity region outer bound can be expressed in terms of the channel parameters and the power constraints. $\qquad\square$

2.3.1 Asymptotic Sum-capacity

As $\mathrm{SNR}_1, \mathrm{SNR}_2, \mathrm{INR} \to \infty$, with their ratios being kept constant, we obtain the following theorem.

Theorem 2. *For the Gaussian three-node full-duplex channel, the asymptotic sum-capacity is established*

$$C_{\mathrm{sum}}^{\mathrm{No\ side-channel}} = \begin{cases} C(\mathrm{SNR}_2) + \mathrm{C}\left(\frac{\mathrm{SNR}_1}{1+\mathrm{INR}}\right) & \mathrm{INR} \leq \mathrm{SNR}_2 \\[2mm] C\left(\mathrm{SNR}_1 + \mathrm{INR}\right) & \mathrm{SNR}_2 \leq \mathrm{INR} \leq \mathrm{SNR}_2(1 + \mathrm{SNR}_1) \\[2mm] C(\mathrm{SNR}_1) + \mathrm{C}(\mathrm{SNR}_2) & \mathrm{INR} \geq \mathrm{SNR}_2(1 + \mathrm{SNR}_1) \end{cases} \tag{2.26}$$

Proof. We only need to prove that the upper bound on the sum-capacity of Gaussian three-node full-duplex channel is tight as $\mathrm{SNR}_1, \mathrm{SNR}_2, \mathrm{INR} \to \infty$. In the weak interference regime where $\mathrm{INR} \leq \mathrm{SNR}_2$, when $\mathrm{SNR}_1, \mathrm{SNR}_2, \mathrm{INR} \to \infty$,

$$\lim_{\substack{\mathrm{SNR}_1, \mathrm{SNR}_2, \\ \mathrm{INR} \to \infty}} \frac{\overline{C}_{\mathrm{sum}}^{\mathrm{No\ side-channel}}}{\underline{C}_{\mathrm{sum}}^{\mathrm{No\ side-channel}}} = \frac{\log(\mathrm{SNR}_2) + \log(\mathrm{INR} + \mathrm{SNR}_1) - \log(\mathrm{INR}) + \log(1 + 2\frac{\sqrt{\bar{\alpha}\mathrm{SNR}_1\mathrm{INR}}}{\mathrm{INR}+\mathrm{SNR}_1})}{\log(\mathrm{SNR}_2) + \log(\mathrm{INR} + \mathrm{SNR}_1) - \log(\mathrm{INR})}$$

$$= 1.$$

The strong interference regime for the sum-capacity lower bound is defined as $\mathrm{SNR}_2 \leq \mathrm{INR} \leq \mathrm{SNR}_2(1 + \mathrm{SNR}_1)$, and the sum-capacity upper bound is defined as

$\text{SNR}_2 \leq \text{INR} \leq \text{INR}^*$, where

$$\text{INR}^* = 2\text{SNR}_1 + \text{SNR}_2(1 + \text{SNR}_1) - 2\sqrt{\text{SNR}_1(\text{SNR}_1 + \text{SNR}_2 + \text{SNR}_1\text{SNR}_2)}$$

. Using L'Hospital's Rule, we can compute

$$\lim_{\substack{\text{SNR}_1,\text{SNR}_2, \\ \text{INR}\to\infty}} \frac{\text{INR}^*}{\text{SNR}_2(1+\text{SNR}_1)} = \lim_{\substack{\text{SNR}_1,\text{SNR}_2, \\ \text{INR}\to\infty}} \frac{2\text{SNR}_1 + \text{SNR}_2(1+\text{SNR}_1) - 2\sqrt{\text{SNR}_1(\text{SNR}_1 + \text{SNR}_2 + \text{SNR}_1\text{SNR}_2)}}{\text{SNR}_2(1+\text{SNR}_1)}$$

$$= 1.$$

Thus in the strong interference regime, according to L'Hospital's Rule, we have

$$\lim_{\text{SNR}_1,\text{SNR}_2,\text{INR}\to\infty} \frac{\overline{C}_{\text{sum}}^{\text{No side-channel}}}{\underline{C}_{\text{sum}}^{\text{No side-channel}}} = \lim_{\text{SNR}_1,\text{SNR}_2,\text{INR}\to\infty} \frac{C\left(\text{SNR}_1 + \text{INR} + 2\sqrt{\text{SNR}_1\text{INR}}\right)}{C\left(\text{SNR}_1 + \text{INR}\right)}$$

$$= 1.$$

$\square$

Therefore, in the high SNR and INR limit, for the Gaussian three-node full-duplex channel, treating interference as noise and joint decoding are asymptotically sum-capacity achieving in weak and strong interference regimes, respectively.

For the ease of analysis, let us consider the symmetric channels where $\text{SNR}_1 = \text{SNR}_2$. We define $\mu = \frac{\log \text{INR}}{\log \text{SNR}}$ to capture the interference level. Hence we can derive the asymptotic multiplexing gain of the sum-capacity over signal-user capacity in the high SNR and INR limit, which is give by

$$M^{\text{No side-channel}} = \frac{C_{\text{sum}}^{\text{No side-channel}}}{C_{\text{awgn}}} = \begin{cases} 2 - \mu & 0 \leq \mu < 1 \\ \mu & 1 \leq \mu < 2 \\ 2 & \mu \geq 2 \end{cases} \tag{2.27}$$

When $\mu = 0$, there is no interference. And $0 \leq \mu < 1$ corresponds to the weak interference regime while $\mu \geq 1$ corresponds to the strong and very strong interference

regimes.

In Fig. 2.2, we compute the asymptotic multiplexing gain of the sum-capacity for the Gaussian three-node full-duplex channel. As delineated in Fig. 2.2, ideally without interference, perfect full-duplex can achieve an multiplexing of 2 in all regimes. When INI is very weak, i.e., μ is slightly greater than zero, the impact of INI is inappreciable because the interference can just be treated as noise. On the other hand, when INI is very strong, i.e., $\mu \geq 2$, the very strong interfering signal can always first be decoded and then subtracted out. However, when INI is neither very weak nor very strong, there exists an area where the full-duplex multiplexing gain vanishes quickly.
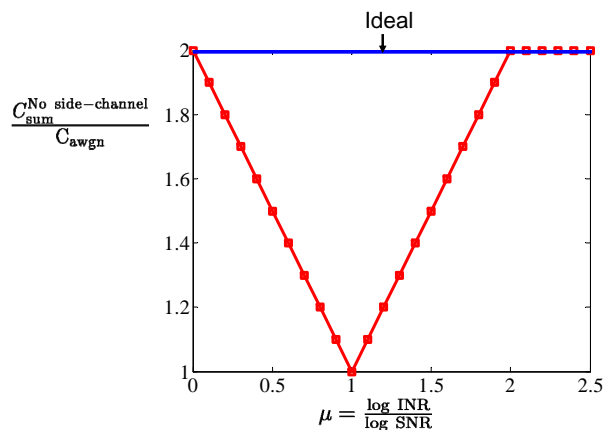
Figure 2.2: Asymptotic multiplexing gain of the sum-capacity for Gaussian three-node full-duplex channel as a function of the interference level μ.

Four Schemes for Side-channel Assisted Three-node Network

In the previous section, we have demonstrated the impact of INI. Therefore, how to alleviate INI is of great importance to increase the multiplexing gain of the three-node full-duplex network. In the three-node network, the inter-node interference is unknown to the unintended receiver of M2 because the transmitter of M1 and interfered receiver of M2 is distributed compared to the known self-interference at the interfered receiver due to co-location of transceiver at full-duplex node.

By extending the use of self-interference cancellation beyond the original co-located transmitter-receiver full-duplex node for bidirectional communication, we propose to leverage a device-to-device side channel for inter-node interference cancellation. The prevalence of multi-ratio interfaces on current mobile devices provides such opportunity to deliver the interfering signal between the two mobile nodes to manage the inter-node interference. We label the protocols for communication in side-channel assisted three-node network as *distributed full-duplex*. In this section, we will propose four distributed full-duplex inter-node interference canellation schemes for improved interference cancellation.

3.1   Bin-and-cancel

The first scheme we propose to leverage the side channel to manage INI is bin-and-cancel, which uses Han-Kobayashi style common-private message splitting. The main idea behind BC scheme is to divide the interfering message of Node M1 into two parts: private message which can only be decoded at the intended receiver Node BS, and common message which can be decoded at both receivers. Then partition the common message of M1 into equal size bins, encode the bin indexes into codewords and send through the side channel. The number of bin indexes is determined by the rate of the side channel. At the interfered receiver M2, by decoding the common message of the interfering signal from M1, part of the interference can be subtracted out while treating the remaining private message of M1 as noise. B By using the side channel, the bin index can first be decoded from the side channel. Then with the help of bin index, the uncertainty of decoding the common message of M1 can be resolved, allowing sending more common message of M1 and mitigating INI. Similar approach is also adopted in [7, 22]. This binning strategy is also capacity-achieving for multiple-access channel with side channel, which is given in the following Lemma.

Lemma 1. *The capacity region of a multiple-access channel with side channel in Fig. 3.1 is*

$$R_1 \leq I(X_1; Y_1 | X_2)$$
$$R_2 \leq I(X_2; Y_1 | X_1) + I(X_3; Y_3)$$
$$R_1 + R_2 \leq I(X_1, X_2; Y_1) + I(X_3; Y_3),$$

for some $p(x_1)p(x_2, x_3)$.

Proof. We first give the outline of achievability.

   1. Codebook generation: Fix $p(x_1)$ and $p_(x_2, x_3)$ that achieves the lower bound.
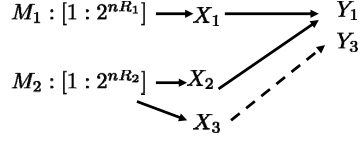
Figure 3.1: Multiple access channel with side channel.

Randomly and independently generate 2^{nR_1} sequence $x_1^n(m_1)$, $m_1 \in [1 : 2^{nR_1}]$, each i.i.d. according to distribution $\prod_{i=1}^n p_{X_1}(x_{1i})$. Randomly and independently generate 2^{nR_3} sequence $x_3^n(l)$, $l \in [1 : 2^{nR_3}]$, each i.i.d. according to distribution $\prod_{i=1}^n p_{X_3}(x_{3i})$. For each l, randomly and conditionally independently generate 2^{nR_2} sequence $x_2^n(m_2|l)$, $m_2 \in [1 : 2^{nR_2}]$, each i.i.d. according to distribution $\prod_{i=1}^n p_{X_2|X_3}(x_{2i}|x_{3i})$. Partition the set $[1 : 2^{nR_2}]$ into 2^{nR_3} equal size bins, $\mathcal{B}(l) = [(l-1)2^{n(R_2-R_3)} + 1 : l2^{n(R_2-R_3)}], l \in [1 : 2^{nR_3}]$. The codebook and bin assignments are revealed to all parties.

2. Encoding: Upon observing $m_2 \in [1 : 2^{nR_2}]$, assign m_2 to bin $\mathcal{B}(l)$. The encoders send $x_1^n(m_1), x_2^n(m_2|l)$ over the main channel, and $x_3^n(l)$ over the side channel in n blocks.

3. Decoding: Upon receiving Y_3, the receiver for the side channel declares that $\hat{l}$ is sent if it is the unique message such that $(x_3^n(\hat{l}), Y_3^n) \in \mathcal{T}_\epsilon^n$; otherwise, it declares an error. Then upon receiving Y_1, the receiver for the main channel declares that $(\hat{m_1}, \hat{m_2})$ are sent if it is the unique pair such that $(x_1^n(\hat{m_1}), x_2^n(\hat{m_2}|\hat{l}), Y_1^n) \in \mathcal{T}_\epsilon^n$ and $\hat{m_2} \in \mathcal{B}(\hat{l})$; otherwise, it declares an error.

Therefore, the following rate region is achievable

$$R_1 \leq I(X_1; Y_1|X_2)$$

$$R_2 \leq I(X_2; Y_1|X_1) + I(X_3; Y_3)$$

$$R_1 + R_2 \leq I(X_1, X_2; Y_1) + I(X_3; Y_3),$$

for some $p(x_1)p(x_2, x_3)$.

The converse comes from cut-set upper bound.

$$
\begin{aligned}
n(R_2) \; &\leq \; I(X_2^n, X_3^n; Y_1^n, Y_3^n | X_1^n) & (3.1)\\
&= \; I(X_2^n; Y_1^n, Y_3^n | X_1^n) + I(X_3^n; Y_1^n, Y_3^n | X_1^n, X_2^n) & (3.2)\\
&= \; I(X_2^n; Y_1^n | X_1^n) + I(X_2^n; Y_3^n | X_1^n, Y_1^n) + H(X_3^n | X_1^n, X_2^n) - H(X_3^n | X_1^n, X_2^n, Y_1^n, Y_3^n) & (3.3)\\
&= \; I(X_2^n; Y_1^n | X_1^n) + I(X_2^n; Y_3^n | X_1^n, Y_1^n) & (3.4)\\
&\leq \; I(X_2^n; Y_1^n | X_1^n) + I(X_3^n; Y_3^n), & (3.5)
\end{aligned}
$$

where (3.4) follows that X_3^n is a function of X_2^n, thus

$$
H(X_3^n | X_1^n, X_2^n) = H(X_3^n | X_1^n, X_2^n, Y_1^n, Y_3^n),
$$

and (3.5) follows that

$$
\begin{aligned}
I(X_2^n; Y_3^n | X_1^n, Y_1^n) &= H(Y_3^n | X_1^n, Y_1^n) - H(Y_3^n | X_1^n, X_2^n, Y_1^n)\\
&\leq H(Y_3^n) - H(Y_3^n | X_3^n) & (3.6)\\
&\leq I(X_3^n | Y_3^n).
\end{aligned}
$$

Similarly, we can also prove that

$$
R_1 \leq I(X_1; Y_1 | X_2)
$$

$$
R_1 + R_2 \leq I(X_1, X_2; Y_1) + I(X_3; Y_3).
$$

For Gaussian MAC with side channel, the above constraints on R_1, R_2 and $R_1 + R_2$ will be simultaneously maximized by Gaussian inputs. □

In the Gaussian channels, assuming all inputs are i.i.d. Gaussian distributed satisfying $X_1 \sim \mathcal{N}(0, P_1)$, $X_{20} \sim \mathcal{N}(0, \bar{\beta}\bar{\lambda}P_2)$, $X_{22} \sim \mathcal{N}(0, \beta\bar{\lambda}P_2)$, and $X_3 \sim \mathcal{N}(0, \lambda P_2)$, respectively, where $\beta, \lambda \in [0, 1], \bar{\beta} + \beta = 1, \bar{\lambda} + \lambda = 1$. The parameter λ denotes

the power allocated to the side channel and β denotes the power being split for the private message of M1. We have the following achievability result.
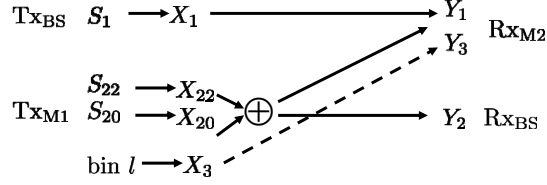
Figure 3.2: Depiction for bin-and-cancel.

Proposition 2. *For Gaussian side-channel assisted three-node network, in the weak interference regime defined by* $\mathrm{INR} \leq \mathrm{SNR}_2$, *the following rate region is achievable for bin-and-cancel,*

$$
\begin{aligned}
R_1 \leq &C\left(\frac{\mathrm{SNR}_1}{1 + \beta\bar{\lambda}\mathrm{INR}}\right) \\
R_2 \leq &\min\left\{C\left(\bar{\lambda}\mathrm{SNR}_2\right), C\left(\beta\bar{\lambda}\mathrm{SNR}_2\right) + C\left(\frac{\bar{\beta}\bar{\lambda}\mathrm{INR}}{1 + \beta\bar{\lambda}\mathrm{INR}}\right)\right. \\
&\left. + WC\left(\frac{\lambda\mathrm{SNR}_{\mathrm{side}}}{W}\right)\right\} \\
R_1 + R_2 \leq &C\left(\beta\bar{\lambda}\mathrm{SNR}_2\right) + C\left(\frac{\mathrm{SNR}_1 + \bar{\beta}\bar{\lambda}\mathrm{INR}}{1 + \beta\bar{\lambda}\mathrm{INR}}\right) + WC\left(\frac{\lambda\mathrm{SNR}_{\mathrm{side}}}{W}\right),
\end{aligned}
\tag{3.7}
$$

where $\beta, \lambda \in [0, 1], \beta + \bar{\beta} = 1, \lambda + \bar{\lambda} = 1$ *and* $C(X) = W_m\log(1 + X)$.

In the strong interference regime defined by $\mathrm{SNR}_2 \leq \mathrm{INR} \leq \mathrm{SNR}_2(1 + \mathrm{SNR}_1)$, *the achievable rate region is*

$$
\begin{aligned}
R_1 \leq &C\left(\mathrm{SNR}_1\right) \\
R_2 \leq &C\left(\bar{\lambda}\mathrm{SNR}_2\right) \\
R_1 + R_2 \leq &C\left(\mathrm{SNR}_1 + \bar{\lambda}\mathrm{INR}\right) + WC\left(\frac{\lambda\mathrm{SNR}_{\mathrm{side}}}{W}\right).
\end{aligned}
\tag{3.8}
$$

In the very strong interference regime defined by $\mathrm{INR} \geq \mathrm{SNR}_2(1 + \mathrm{SNR}_1)$, *the*

capacity region is

$$R_1 \leq C\left(\text{SNR}_1\right)$$

$$R_2 \leq C\left(\text{SNR}_2\right)$$

(3.9)

Proof. The encoding procedure is depicted in Figure 3.2. Using the Han-Kobayashi common-private message splitting strategy, the common message can be decoded at both receivers, while private message can only be decoded at the intended receiver. Message S_1 is of size 2^{nR_1}, and X_1 is intended to be decoded at Y_1 only. Message S_2 is divided into common part S_{20} of size $2^{nR_{20}}$, and private part S_{22} of size $2^{nR_{22}}$. Superpose the codewords of both S_{22} and S_{20} such that $X_2 = X_{20} + X_{22}$. Then partition the set $[1 : 2^{nR_{20}}]$ into 2^{nR_3} equal size bins, $\mathcal{B}(l) = [(l-1)2^{n(R_{20}-R_3)} + 1 : l2^{n(R_{20}-R_3)}], l \in [1 : 2^{nR_3}]$, and $X_3(l)$ is sent through the side channel.

Decoding occurs in two steps. Upon receiving $Y_2, (X_{20}, X_{22})$ are first decoded. The set of achievable rates (R_{20}, R_{22}) is the capacity region of a multiple-access channel denoted as $\mathcal{C}_1$, where

$$R_{20} \leq I(X_{20}; Y_2 | X_{22})$$

$$R_{22} \leq I(X_{22}; Y_2 | X_{20})$$

$$R_{20} + R_{22} \leq I(X_{20}, X_{22}; Y_2),$$

(3.10)

for some distribution product $p(x_{20})p(x_{22})$.

Then upon receiving Y_1, Y_3, with the help of the side channel (X_1, X_{20}) are decoded treating X_{22} as noise. This is a multiple-access channel with side channel. The capacity region of such channel denoted as $\mathcal{C}_2$ is established, which is proved in

Lemma 1. Thus we have

$$R_1 \leq I(X_1; Y_1 | X_{20})$$

$$R_{20} \leq I(X_{20}; Y_1 | X_1) + I(X_3; Y_3) \tag{3.11}$$

$$R_1 + R_{20} \leq I(X_1, X_{20}; Y_1) + I(X_3; Y_3),$$

for some distribution product $p(x_1)p(x_{20}, x_3)$.

In the Gaussian channels, we first split the total transmit power of Node M1 between side channel and main channel, then split the power allocated to the main channel between the common and private message. Thus when the inputs are i.i.d. Gaussian distributed satisfying $X_1 \sim \mathcal{N}(0, P_1), X_{20} \sim \mathcal{N}(0, \bar{\beta}\bar{\lambda}P_2), X_{22} \sim \mathcal{N}(0, \beta\bar{\lambda}P_2)$, and $X_3 \sim \mathcal{N}(0, \lambda P_2)$, respectively, where $\beta, \lambda \in [0, 1], \bar{\beta} + \beta = 1, \bar{\lambda} + \lambda = 1$, we can obtain the achievable rate region by substituting channels parameters and power constraints into (3.10) and (3.11). □

Remark 1. *In the weak interference regime, BC scheme contributes to improving the downlink rate R_1 which is limited by the interference from M1. While in the strong interference regime where $\mathrm{INR} \geq \mathrm{SNR}_2$, M1 sends all common message, and there is no interference at the receiver of M2. In this case, BC scheme enables M1 to deliver more common message which is restricted by the interference link, thus increasing the uplink rate R_2.*

BC scheme adopts Han-Kobayashi strategy which allows arbitrary splits of total transmit power between common message and private message in the weak interference regime in addition to the power split between the side channel and main channel. Therefore, the optimization among such myriads of possibilities is hard in general. We can simplify BC scheme by setting power splitting of private message of M1 at the level of Gaussian noise at the receiver of M2 in the weak interference regime. Namely, let the power for the private message S_{22} of M1 satisfy $\mathrm{INR}_p = \beta\bar{\lambda}\mathrm{INR} = 1$.

This particular simple common-private power splitting is used in [12] and is shown to achieve to within one bit of the capacity region of the general two-user interference channel. We will use this simplified BC scheme for the capacity analysis.

3.2 Three Simpler Schemes

We propose three simpler schemes compared to BC scheme for encoding X_3 and sequentially post-processing (Y_1, Y_3) at Receiver M2. The first is compress-and-cancel, which simplifies the transmitter design of Node M1. Then we give another two schemes: decode-and-cancel and estimate-and-cancel, both of which not only simplify the transmitter design of M1, but also the receiver design of M2.

3.2.1 Compress-and-cancel

As shown in Fig. 3.3, for compress-and-cancel scheme, the transmitter design of M1 is simplified compared to BC scheme. Node M1 just sends a compressed version of the interfering message over the side channel using source coding. Noticing that the correlated information with the interfering message can be observed at receiver M2, Wyner-Ziv strategy [21] can be adopted for compression. We first compress X_2 into $\widehat{X_2}$, then encode $\widehat{X_2}$ as X_3 and transmit over the side channel. At the receiver M2, with the knowledge of the distribution of Y_1, we can recover the interference under certain distortion and subtract it from the main channel. The capacity of the side channel should allow reliable transmission of the compressed signal $\widehat{X_2}$.

In the Gaussian channels, all inputs are assumed to be i.i.d. Gaussian distributed, satisfying $X_1 \sim \mathcal{N}(0, P_1), X_2 \sim \mathcal{N}(0, \bar{\lambda} P_2)$ and $X_3 \sim \mathcal{N}(0, \lambda P_2)$, respectively, where $\lambda \in [0, 1], \bar{\lambda} + \lambda = 1$. For the ease of analysis, we also assume $\widehat{X_2}$ to be a Gaussian
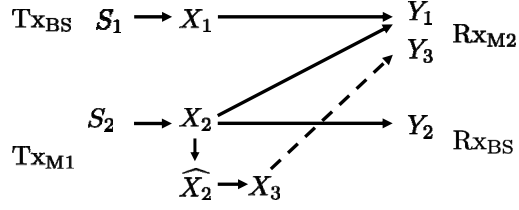
Figure 3.3: Depiction of compress-and-cancel.

quantized version of X_2:

$$\widehat{X_2} = X_2 + Z_q, \tag{3.12}$$

where Z_q is the quantization noise with Gaussian distribution $\mathcal{N}(0, \sigma_q^2)$. We can obtain the following inner bound,

Proposition 3. *For Gaussian side-channel assisted three-node network, the following rate region is achievable for compress-and-cancel*

$$R_1 \leq C \left(\frac{\text{SNR}_1 \left(1 + \text{SNR}_1 + (1 + \text{SNR}_1 + \bar{\lambda}\text{INR})[(1 + \frac{\lambda\text{SNR}_{\text{side}}}{W})^W - 1]\right)}{(1 + \text{SNR}_1 + \bar{\lambda}\text{INR})[(1 + \frac{\lambda\text{SNR}_{\text{side}}}{W})^W - 1] + (1 + \text{SNR}_1)(1 + \bar{\lambda}\text{INR}))} \right)$$

$$R_2 \leq C \left(\bar{\lambda}\text{SNR}_2 \right).$$

$$\tag{3.13}$$

Proof. For compress-and-cancel scheme, the achievable rate region is given by

$$R_1 \leq I(X_1; Y_1, \widehat{X_2})$$

$$R_2 \leq I(X_2; Y_2) \tag{3.14}$$

$$\text{S.t. } I(X_2; \widehat{X_2}|Y_1) \leq I(X_3; Y_3),$$

for distribution product $p(x_1)p(x_2)p(x_3)p(\widehat{x}_2|x_2, y_1)$.

We have

$$
\begin{aligned}
R_{\hat{X}_2|Y_1} = I(X_2; \hat{X}_2|Y_1) &\leq I(X_3; Y_3) \\
&= h(\hat{X}_2|Y_1) - h(\hat{X}_2|Y_1, X_2) \leq I(X_3; Y_3) \\
&= W_m \log\left(1 + \frac{\bar{\lambda}P_2(\gamma_1 P_1 + \sigma^2)}{(\gamma_1 P_1 + \gamma_{21}\bar{\lambda}P_2 + \sigma^2)\sigma_q^2}\right) \leq W_s \log\left(1 + \frac{\gamma_3 \lambda P_2}{W\sigma^2}\right),
\end{aligned} \tag{3.15}
$$

thus we can obtain

$$
\sigma_q^2 \geq \frac{\bar{\lambda}P_2(\gamma_1 P_1 + \sigma^2)}{(\gamma_1 P_1 + \gamma_{21}\bar{\lambda}P_2 + \sigma^2)[(1 + \frac{\gamma_3 \lambda P_2}{W\sigma^2})^W - 1]}. \tag{3.16}
$$

And

$$
\begin{aligned}
R_1 &\leq I(X_1; Y_1, \hat{X}_2) \\
&= W_m \log\left(1 + \frac{\gamma_1 P_1(\bar{\lambda}P_2 + \sigma_q^2)}{\gamma_{21}\bar{\lambda}P_2\sigma_q^2 + \sigma^2(\bar{\lambda}P_2 + \sigma_q^2)}\right).
\end{aligned} \tag{3.17}
$$

Since R_1 is a decreasing function of σ_q^2, now we can calculate R_1 by substituting (3.16) into (3.17). And R_2 is given by

$$
\begin{aligned}
R_2 &\leq I(X_2; Y_2) \\
&= C\left(\bar{\lambda}\mathrm{SNR}_2\right).
\end{aligned} \tag{3.18}
$$

$\square$

3.2.2 Decode-and-cancel

Decode-and-cancel can lead to a simpler transceiver design for M1 compared to BC scheme where no common-private message splitting is adopted at the transmitter of M1, and only single-user decoders are involved at the receiver of M2. In DC scheme,

the interfering message S_2 of Node M1 is encoded into two codewords using two independent Gaussian codebooks. Then the two codewords are sent, one through the main channel and the other through the side channel. The message S_2 is required to be decoded at both the intended receiver of BS and the side-channel receiver of M2. After decoding S_2 from the side channel, the interference can be cancelled out at the main-channel receiver of M2.

In the Gaussian channels, all inputs are assumed to be i.i.d. Gaussian distributed, satisfying $X_1 \sim \mathcal{N}(0, P_1), X_2 \sim \mathcal{N}(0, \bar{\lambda}P_2)$ and $X_3 \sim \mathcal{N}(0, \lambda P_2)$, respectively, where $\lambda \in [0, 1], \bar{\lambda} + \lambda = 1$. The parameter λ denotes the power allocated to the side channel. We obtain the following inner bound achieved by DC.

Proposition 4. *(from [1]) For Gaussian side-channel assisted three-node network, the following rate region is achievable for decode-and-cancel*

$$
\begin{aligned}
R_1 &\leq C_1 \\
R_2 &\leq \min\left\{ WC\left(\frac{\lambda\mathrm{SNR_{side}}}{W}\right), C\left(\bar{\lambda}\mathrm{SNR_2}\right)\right\}.
\end{aligned}
\tag{3.19}
$$

The decode-and-cancel scheme can also be improved by adopting Han-Koybayashi common-private message splitting. The private message of M1 is encoded into two independent codewords and sent over main channel and side channel. The private message of M1 is required to be decoded from the side channel in addition to its own intended receiver. After decoding the private message of M1 from the side channel, the interference from the private part of M1 is cancelled out from the main channel.

When the inputs are i.i.d. Gaussian distributed satisfying $X_1 \sim \mathcal{N}(0, P_1), X_{20} \sim \mathcal{N}(0, \bar{\beta}\bar{\lambda}P_2)$, $X_{22} \sim \mathcal{N}(0, \beta\bar{\lambda}P_2)$, and $X_3 \sim \mathcal{N}(0, \lambda P_2)$, respectively, we have the results below.

Proposition 5. *For Gaussian three-node full-duplex with side channel, the following rate region is achievable for decode-and-cancel with Han-Koybayashi common-private*

message splitting

$$R_1 \leq C\left(\mathrm{SNR}_1\right)$$

$$R_2 \leq \min\left\{C\left(\beta\bar{\lambda}\mathrm{SNR}_2\right), WC\left(\frac{\lambda\mathrm{SNR}_{\mathrm{side}}}{W}\right)\right\} + \tag{3.20}$$
$$\min\left\{C\left(\frac{\bar{\beta}\bar{\lambda}\mathrm{INR}}{1+\mathrm{SNR}_1}\right), C\left(\frac{\bar{\beta}\bar{\lambda}\mathrm{INR}}{1+\beta\bar{\lambda}\mathrm{SNR}_2}\right)\right\}.$$

where $\beta + \bar{\beta} = 1, \beta \in [0,1]$.

When $\beta = 1$, i.e., M1 sends all private message, (3.20) will reduce to (3.19).

3.2.3 Estimate-and-cancel

We also propose an estimate-and-cancel scheme which is even simpler than DC scheme. In estimate-and-cancel, Node M1 will send a scaled version of the waveform of the interfering signal over the side channel. We estimate the received waveform Y_3 from side channel, rescale it according to X_2 and cancel it out from Y_1. Then the signal-of-interest can be decoded from its single-user decoder. But in EC scheme, we have less flexibility in using the side channel since the bandwidth of the side channel is required to be equal or larger than that of the main channel. Let $X_3 = KX_2$, where K is a scalar $(K \geq 0)$ satisfying the per-node power constraint, i.e., $\mathbb{E}(|X_2 + X_3|^2) \leq P_2$. Thus $\mathbb{E}(|X_2|^2) \leq \frac{P_2}{(1+K)^2}$.

We adopt independently Gaussian codebooks for X_1 and X_2 with $X_1 \sim \mathcal{N}(0, P_1), X_2 \sim \mathcal{N}\left(0, \frac{P_2}{(1+K)^2}\right)$. Side-channel signal X_3 is correlated with X_2 with $X_3 \sim \mathcal{N}\left(0, \frac{K^2 P_2}{(1+K)^2}\right)$, and correlation coefficient $\rho = 1$, where $K \geq 0$. The resulting rate of EC is given as follows,

Proposition 6. *For Gaussian side-channel assisted three-node network, the following*

rate region is achievable for estimate-and-cancel

$$
\begin{aligned}
R_1 &\leq C\left(\frac{\mathrm{SNR}_1\left(1 + \frac{K^2\mathrm{SNR}_{\mathrm{side}}}{(1+K)^2}\right)}{1 + \frac{K^2\mathrm{SNR}_{\mathrm{side}}}{(1+K)^2} + \frac{\mathrm{INR}}{(1+K)^2}}\right)\\
R_2 &\leq C\left(\frac{\mathrm{SNR}_2}{(1+K)^2}\right),
\end{aligned}
\tag{3.21}
$$

where $K \geq 0$.

Proof. For Gaussian channels, by substituting the channel parameters and power constraint, the achievable rate region can be calculated

$$
\begin{aligned}
R_1 &\leq I(X_1; Y_1, Y_3)\\
&= h(Y_1, Y_3) - h(Y_1, Y_3 | X_1)\\
&= C\left(\frac{\mathrm{SNR}_1\left(1 + \frac{K^2\mathrm{SNR}_{\mathrm{side}}}{(1+K)^2}\right)}{1 + \frac{K^2\mathrm{SNR}_{\mathrm{side}}}{(1+K)^2} + \frac{\mathrm{INR}}{(1+K)^2}}\right)\\
R_2 &\leq I(X_2; Y_2)\\
&= C\left(\frac{\mathrm{SNR}_2}{(1+K)^2}\right).
\end{aligned}
\tag{3.22}
$$

$\square$

Remark 2. *The achievable rate region of EC can be improved by optimizing the correlation coefficient between X_2 and X_3. If the correlation between X_2 and X_3 is higher, then less power can be allocated for the side channel due to the per-node power constraint. Since there is a tradeoff between finding the the correlation coefficient and the power splitting for the side channel signal, the optimization problem becomes harder to find the all possible solutions.*

Bounds on Capacity Region of Side-channel Assisted Three-node Network

4.1 New Outer Bound

In this section, we derive a new outer bound to characterize the performance of the four schemes discussed in Sections 3.1 and 3.2. When there is no INI in the side-channel assisted three-node full-duplex network, we can obtain the no-interference outer bound,

$$
\begin{aligned}
R_1 &\leq C\left(\mathrm{SNR}_1\right) \\
R_2 &\leq C\left(\mathrm{SNR}_2\right).
\end{aligned}
\tag{4.1}
$$

However, the no-interference outer bound can be arbitrarily loose. We notice that one of the transmitter and receiver pairs in Figure 2.1 is co-located at the base station, thus causal information of M1 is available at the transmitter of BS. Hence we derive a new outer bound on the capacity region of Gaussian side-channel assisted three-node network as follows.

Theorem 3. *For Gaussian side-channel assisted three-node network under per-node*

power constraint, the capacity outer bound in the weak interference regime, i.e., $\text{INR} \leq$ SNR_2 *is given by*

$$R_1 \leq C\left(\text{SNR}_1\right)$$

$$R_2 \leq C\left(\bar{\lambda}\text{SNR}_2\right)$$

$$R_1 + R_2 \leq C\left(\frac{\bar{\alpha}\bar{\lambda}\text{INR} + \text{SNR}_1 + 2\sqrt{\bar{\alpha}\bar{\lambda}\text{SNR}_1\text{INR}}}{1 + \alpha\bar{\lambda}\text{INR}}\right) + C\left(\alpha\bar{\lambda}\text{SNR}_2\right) + WC\left(\frac{\lambda\text{SNR}_{\text{side}}}{W}\right).$$

$$(4.2)$$

The capacity outer bound in the strong interference regime, i.e., $\text{INR} \geq \text{SNR}_2$ *is given by*

$$R_1 \leq C\left(\text{SNR}_1\right)$$

$$R_2 \leq C\left(\bar{\lambda}\text{SNR}_2\right) \tag{4.3}$$

$$R_1 + R_2 \leq C\left(\text{SNR}_1 + \bar{\lambda}\text{INR} + 2\sqrt{\bar{\lambda}\text{SNR}_1\text{INR}}\right) + WC\left(\frac{\lambda\text{SNR}_{\text{side}}}{W}\right),$$

where $\alpha, \lambda \in [0,1], \alpha + \bar{\alpha} = 1, \lambda + \bar{\lambda} = 1.$

Proof. The bounds on R_1 and R_2 come from the point-to-point capacity of AWGN channel. The bound on $R_1 + R_2$ is the sum-rate of Gaussian side-channel assisted Z channel. Messages S_1 and S_2 are chosen uniformly and independently at random, and X_{1i} is a function of (S_1, Y_2^{i-1}). We define $U_i = (S_1, Y_2^{i-1}, X_1^{i-1})$ for $i \in [1, n]$. From Fano's inequality, we have $H(S_i|Y_i^n) \leq \epsilon_n$ for $i = 1, 2$, where n goes to infinity

as ϵ_n goes to zero. By Fano's inequality, for any codebook of block length n,

$$
\begin{aligned}
nR_1 \quad &\leq \quad I(S_1; Y_1^n, Y_3^n) + n\epsilon_1 \quad &(4.4)\\
&= \quad I(S_1; Y_1^n) + I(S_1; Y_3^n | Y_1^n) + n\epsilon_1 \quad &(4.5)\\
&= \quad I(S_1; Y_1^n) + H(Y_3^n | Y_1^n) - H(Y_3^n | Y_1^n, S_1) + n\epsilon_1 \quad &(4.6)\\
&\leq \quad I(S_1; Y_1^n) + I(X_3^n; Y_3^n) + n\epsilon_1 \quad &(4.7)\\
&\leq \quad \sum_{i=1}^{n} I(S_1, Y_1^{i-1}; Y_{1i}) + \sum_{i=1}^{n} I(X_{3i}; Y_{3i}) + n\epsilon_1 \quad &(4.8)\\
&\leq \quad \sum_{i=1}^{n} I(S_1, Y_2^{i-1}, Y_1^{i-1}; Y_{1i}) + \sum_{i=1}^{n} I(X_{3i}; Y_{3i}) + n\epsilon_1 \quad &(4.9)\\
&= \quad \sum_{i=1}^{n} I(S_1, Y_2^{i-1}, X_1^i, Y_1^{i-1}; Y_{1i}) + \sum_{i=1}^{n} I(X_{3i}; Y_{3i}) + n\epsilon_1 \quad &(4.10)\\
&= \quad \sum_{i=1}^{n} I(S_1, Y_2^{i-1}, X_1^i; Y_{1i}) + \sum_{i=1}^{n} I(X_{3i}; Y_{3i}) + n\epsilon_1 \quad &(4.11)\\
&= \quad \sum_{i=1}^{n} I(U_i, X_{1i}; Y_{1i}) + \sum_{i=1}^{n} I(X_{3i}; Y_{3i}) + n\epsilon_1, \quad &(4.12)
\end{aligned}
$$

where (4.7) follows from $H(Y_3^n | Y_1^n) \leq H(Y_3^n)$ and $-H(Y_3^n | Y_1^n, S_1) \leq -H(Y_3^n | X_3^n)$; (4.10) and (4.12) follow because X_{1i} is a function of (S_1, Y_2^{i-1}); (4.11) follows because $Y_1^{i-1} \to (X_1^i, Y_2^{i-1}) \to Y_{1i}$ forms a Markov chain. And for any codebook of block

length n , we have

$$nR_2 = H(S_2|S_1) \tag{4.13}$$

$$= I(S_2; Y_2{}^n|S_1) + H(S_2|Y_2^n, S_1) \tag{4.14}$$

$$\leq I(S_2; Y_2{}^n|S_1) + n\epsilon_2 \tag{4.15}$$

$$= \sum_{i=1}^{n} I(S_2; Y_{2i}|Y_2^{i-1}, S_1) + n\epsilon_2 \tag{4.16}$$

$$= \sum_{i=1}^{n} I(S_2, Y_{2i}|Y_2^{i-1}, S_1, X_1^i) + n\epsilon_2 \tag{4.17}$$

$$\leq \sum_{i=1}^{n} I(X_{2i}, Y_{2i}|U_i, X_{1i}) + n\epsilon_2, \tag{4.18}$$

where (4.15) follows from Fano's inequality; (4.17) follows because X_{1i} is a function of (S_1, Y_2^{i-1}).

Now by applying the standard time sharing argument, we can obtain

$$R_1 + R_2 \leq I(U, X_1; Y_1) + I(X_2, Y_2|U, X_1) + I(X_3; Y_3), \tag{4.19}$$

for product distribution $p(u)p(x_1x_2x_3|u)p(y_1y_2|x_1x_2x_3)$.

Similarly, in the strong interference regime where $I(X_2; Y_2|X_1, U) \leq I(X_2; Y_1|X_1, U)$, the sum-capacity upper bound is given by

$$R_1 + R_2 \leq I(U, X_1; Y_1) + I(X_2, Y_2|U, X_1) + I(X_3; Y_3) \tag{4.20}$$

$$\leq I(U, X_1; Y_1) + I(X_2, Y_1|U, X_1) + I(X_3; Y_3)$$

$$= I(U, X_1, X_2; Y_1) + I(X_3; Y_3).$$

In the Gaussian channels, the capacity region is upper bounded by Gaussian inputs. The auxiliary random variable U captures the correlation between the code-

words X_1 and X_2. We define $\alpha = 1 - \rho^2$, where ρ is the correlation coefficient between X_1 and X_2 and $\alpha \in [0, 1]$. With per-node power constraint, i.e., $\mathbb{E}(|X_1|^2) \leq P_1$, $\mathbb{E}(|X_2 + X_3|^2) \leq P_2$, let power allocated to the side channel be $\mathbb{E}(|X_3|^2) = \lambda P_2$, thus we have $\mathbb{E}(|X_2|^2) \leq \bar{\lambda} P_2$, where $\lambda \in [0, 1], \bar{\lambda} + \lambda = 1$. Hence the capacity region outer bound can be expressed in terms of parameters α, λ, channel coefficient and per-node power constraints. $\qquad\square$

4.2 Within One Bit of the Capacity Region

So far, we have explained how to leverage the side channel with four distributed full-duplex interference cancellation schemes, and in this section we will show how close can our proposed schemes get to the capacity region.

Let $\mathcal{R}_{\mathrm{BC}} = \bigcup_{\beta,\lambda} \mathfrak{R}_{\mathrm{BC}}(\beta, \lambda)$ denote the achievable rate region for bin-and-cancel including all possible power split at Node M1, where $\mathfrak{R}_{\mathrm{BC}}(\beta, \lambda)$ denote the achievable rate region for a fixed power split between common and private information of M1, as well as side channel and main channel at M1. The main result is given in the following theorem.

Theorem 4. *The achievable region $\mathcal{R}_{\mathrm{BC}}$ is within 1 bit/s/Hz of the capacity region of Gaussian side-channel assisted three-node network, for all values of channel parameters and bandwidth ratio.*

Proof. Let $\delta_{R_1}^{\mathrm{BC}}$ denote the difference between the upper bound on R_1 and achievable rate R_1 in $\mathcal{R}_{\mathrm{BC}}$. Likewise, we have $\delta_{R_2}^{\mathrm{BC}}$ and $\delta_{R_1+R_2}^{\mathrm{BC}}$, where all rates are divided by the total bandwidth $W_m + W_s$. In order to prove the rate pair $(R_1 - 1, R_2 - 1)$ in $\mathcal{R}_{\mathrm{BC}}$ is achievable for any (R_1, R_2) in the capacity region of Gaussian three-node full-duplex

with side channel, we just need to show that

$$\delta_{R_1}^{\mathrm{BC}} < 1$$

$$\delta_{R_2}^{\mathrm{BC}} < 1 \tag{4.21}$$

$$\delta_{R_1+R_2}^{\mathrm{BC}} < 2.$$

Since the upper bound in the weak interference regime is different from that in the strong interference regime. We will prove (4.21) for two different cases.

1. In the weak interference regime where $\mathrm{INR} \leq \mathrm{SNR}_2$, we use the simplified BC scheme for comparison when the power splitting of private message of M1 is set at the level of Gaussian noise at the receiver of M2, i.e., $\mathrm{INR}_p = \beta \bar{\lambda} \mathrm{INR} = 1$. Thus $\mathfrak{R}_{\mathrm{BC}}(\beta = \frac{1}{\bar{\lambda} \mathrm{INR}}) \subset \mathfrak{R}_{\mathrm{BC}}$. We can compute $\mathfrak{R}_{\mathrm{BC}}(\beta = \frac{1}{\bar{\lambda} \mathrm{INR}})$ directly from Proposition 2, by comparing with the new outer bound in (4.2), it is straightforward to show that

$$
\begin{aligned}
\delta_{R_1}^{\mathrm{BC}} &\leq \frac{W_m}{W_m + W_s} \log\left(1 + \frac{\mathrm{SNR}_1}{2 + \mathrm{SNR}_1}\right) \\
&< \frac{1}{1+W} \leq 1 \\
\delta_{R_2}^{\mathrm{BC}} &\leq \frac{W_m}{W_m + W_s} \max\left\{0, 1 + \log\left(\frac{1 + \bar{\lambda}\mathrm{SNR}_2}{1 + \bar{\lambda}\mathrm{INR}} \frac{\mathrm{INR}}{\mathrm{INR} + \mathrm{SNR}_2}\right) \right. \\
&\left. \quad - W \log\left(1 + \frac{\lambda \mathrm{SNR}_{\mathrm{side}}}{W}\right)\right\} \\
&< \frac{1}{1+W} \leq 1 \\
\delta_{R_1+R_2}^{\mathrm{BC}} &\leq \frac{W_m}{W_m + W_s}\left(1 + \log\left(1 + \frac{2\sqrt{\alpha\bar{\lambda}\mathrm{SNR}_1\mathrm{INR}}}{1 + \mathrm{SNR}_1 + \bar{\lambda}\mathrm{INR}}\right)\right. \\
&\left. \quad + \log\left(\frac{1 + \alpha\bar{\lambda}\mathrm{SNR}_2}{1 + \alpha\bar{\lambda}\mathrm{INR}} \frac{\mathrm{INR}}{\mathrm{INR} + \mathrm{SNR}_2}\right)\right) \\
&< \frac{2}{1+W} \leq 2.
\end{aligned}
\tag{4.22}
$$

2. In the strong interference regime where $\mathrm{INR} \geq \mathrm{SNR}_2$, by substituting the outer

bound in (4.3) and inner bound achieved by BC in (3.8), we have

$$\delta_{R_1}^{\mathrm{BC}} = 0$$

$$\delta_{R_2}^{\mathrm{BC}} = 0 \tag{4.23}$$

$$\delta_{R_1+R_2}^{\mathrm{BC}} \leq \frac{W_m}{W_m + W_s} \log\left(1 + \frac{2\sqrt{\bar{\lambda}\mathrm{SNR}_1\mathrm{INR}}}{1 + \mathrm{SNR}_1 + \bar{\lambda}\mathrm{INR}}\right) \leq \frac{1}{1 + W} \leq 1.$$

In the strong interference regime, BC can achieve within half bit of the capacity region.

$\square$

We also characterize the capacity gap for two simpler schemes, DC and EC, and the following theorem quantifies the conditions where DC and EC can achieve within half bit of the capacity region, respectively.

Theorem 5. *1. For decode-and-cancel, the achievable region $\mathcal{R}_{\mathrm{DC}}$ is within $\frac{1}{2}$ bits/s/Hz of the capacity region of Gaussian side-channel assisted three-node network when $W \geq 1$, $\mathrm{SNR}_{\mathrm{side}} \geq \mathrm{SNR}_2$.*

2. For estimate-and-cancel, the achievable region $\mathcal{R}_{\mathrm{EC}}$ is within $\frac{1}{2}$ bits/s/Hz of the capacity region of Gaussian side-channel assisted three-node network when $W \in \mathbb{N}^+$ and $\mathrm{SNR}_{\mathrm{side}} \geq \left(1 + \frac{2}{\sqrt{2}-1}\right) \mathrm{INR}$.

Proof. 1. We first prove the condition on half bit capacity gap for DC scheme. It is not difficult to find that the achievable rate of DC is an increasing function of W. When $W \geq 1$, according to [1], $R_2 \geq C\left(\frac{\mathrm{SNR}_2\mathrm{SNR}_{\mathrm{side}}}{\mathrm{SNR}_2+\mathrm{SNR}_{\mathrm{side}}}\right)$. Hence when $W \geq 1$, $\mathrm{SNR}_{\mathrm{side}} \geq \mathrm{SNR}_2$, comparing with the no-interference outer bound in

(4.1) we can prove that

$$
\delta_{R_1}^{\mathrm{DC}} = 0
$$

$$
\begin{aligned}
\delta_{R_2}^{\mathrm{DC}} &\leq \frac{W_m}{W_m + W_s}\log\left(1 + \mathrm{SNR}_2\right) - \frac{W_m}{W_m + W_s}\log\left(\frac{\mathrm{SNR}_2 \mathrm{SNR}_{\mathrm{side}}}{\mathrm{SNR}_2 + \mathrm{SNR}_{\mathrm{side}}}\right) \\
&= \frac{W_m}{W_m + W_s}\log\left(1 + \frac{\mathrm{SNR}_2^2}{\mathrm{SNR}_2 + \mathrm{SNR}_{\mathrm{side}} + \mathrm{SNR}_2 \mathrm{SNR}_{\mathrm{side}}}\right) \\
&\leq \frac{1}{1 + W} \leq \frac{1}{2}
\end{aligned}
\tag{4.24}
$$

2. For EC scheme, the bandwidth ratio between side channel and main channel is required to be greater than 1, i.e., $W \geq 1$. Comparing rates of EC in Proposition 6 with the no-interference outer bound we have

$$
\begin{aligned}
\delta_{R_1}^{\mathrm{EC}} &\leq \frac{W_m}{W_m + W_s}\log\left(1 + \mathrm{SNR}_1\right) - \frac{W_m}{W_m + W_s}\log\left(1 + \frac{\mathrm{SNR}_1\left(1 + \frac{K^2 \mathrm{SNR}_{\mathrm{side}}}{(1+K)^2}\right)}{1 + \frac{K^2 \mathrm{SNR}_{\mathrm{side}}}{(1+K)^2} + \frac{\mathrm{INR}}{(1+K)^2}}\right) \\
&= \frac{W_m}{W_m + W_s}\log\left(1 + \frac{\frac{\mathrm{SNR}_1 \mathrm{INR}}{(1+K)^2}}{1 + \frac{K^2 \mathrm{SNR}_{\mathrm{side}}}{(1+K)^2} + \frac{\mathrm{INR}}{(1+K)^2} + \mathrm{SNR}_1\left(1 + \frac{K^2 \mathrm{SNR}_{\mathrm{side}}}{(1+K)^2}\right)}\right) \\
\delta_{R_2}^{\mathrm{EC}} &\leq \frac{W_m}{W_m + W_s}\log\left(1 + \mathrm{SNR}_2\right) - \frac{W_m}{W_m + W_s}\log\left(1 + \frac{\mathrm{SNR}_2}{(1+K)^2}\right) \\
&= \frac{W_m}{W_m + W_s}\log\left(1 + \frac{\frac{K(K+2)\mathrm{SNR}_2}{(1+K)^2}}{1 + \frac{\mathrm{SNR}_2}{(1+K)^2}}\right).
\end{aligned}
\tag{4.25}
$$

The achievable rate region of EC is the union of rate pairs for all possible values of K, where $K \geq 0$. Therefore, when $\mathrm{SNR}_{\mathrm{side}} \geq \left(1 + \frac{2}{\sqrt{2}-1}\right)\mathrm{INR}$, and we chose $K = \sqrt{2} - 1$, the following inequalities will hold simultaneously

$$
\begin{aligned}
\delta_{R_1}^{\mathrm{EC}} &\leq \frac{1}{1 + W} \leq \frac{1}{2} \\
\delta_{R_2}^{\mathrm{EC}} &\leq \frac{1}{1 + W} \leq \frac{1}{2}.
\end{aligned}
\tag{4.26}
$$

$\square$

4.3 Discussion of capacity analysis results

Practical communication systems usually operate in the inference-limited regime, so the strength of the signal and interference are much larger than the thermal noise. Our one-bit capacity gap result shows that for all channel parameters and bandwidth ratio, BC scheme is asymptotic optimal in high SNR, INR limit, because one bit is relatively small compared to the rate of the users. And in high SNR, the achievable rate region of BC is a good approximation of the capacity for Gaussian side-channel assisted three-node network. For the two simple schemes, DC and EC can achieve the near-optimal (half-bit gap) performance only in certain regimes of channel values. From the capacity analysis in previous section, we can also find out that the capacity gap for each scheme is inversely proportional to the bandwidth ratio W, where $W \in [0, W_{\max}]$. Often, in practical wireless communication, the bandwidth of side channel is different from the main channel. For example, ISM band radio can operate on a bandwidth up to 80 MHz in 2.4 GHz. In contrast, generally the bandwidth of current 3G/4G radio is 20 MHz. Motivated by the application of leveraging ISM band as the side channel in a cellular network, the bandwidth of side channel usually is much larger than that of main channel. If $W = W_{\max}$, for all values of SNR and INR, BC is near-optimal which achieves within $\frac{1}{1+W_{\max}}$ bits/s/Hz of the capacity region.

Performance Comparisons of Proposed Schemes by Leveraging a Device-to-Device Side Channel

5.1 Finite SNR Multiplexing Gain and Optimal Power Allocation

For simplicity, we assume $\mathrm{SNR}_1 = \mathrm{SNR}_2 = \mathrm{SNR}$ and we define $\mu = \frac{\log \mathrm{INR}}{\log \mathrm{SNR}}$, $\nu = \frac{\log \mathrm{SNR}_{\mathrm{side}}}{\log \mathrm{SNR}}$. Parameter μ captures the interference level, parameters ν and $\frac{\nu}{\mu}$ capture the side channel level compared with main channel. In this paper, we use multiplexing gain as the metric to characterize the rate improvement by leveraging the side channel which is given as

$$M = \frac{R_{\mathrm{sum}}(\mathrm{SNR}, \mathrm{INR})}{C_{\mathrm{single-user}}(\mathrm{SNR})}, \tag{5.1}$$

where $C_{\mathrm{single-user}} = W_m \log(1 + \mathrm{SNR})$. The single-user capacity is the maximum uplink/downlink rate in the three-node network. Ideally, a perfect full-duplex can achieve the maximum multiplexing gain of 2 when there is no interference.

In this section, we will characterize the performance of the schemes proposed in

Chapter 3 for finite SNR values. Fig. 5.1 depicts the multiplexing gain of each scheme when SNR=15 dB, $W = 1$ and $\nu = \mu$. Fig. 5.2 shows the corresponding optimal power allocated to the side channel which maximizes achievable sum-rate of each proposed schemes. In Fig. 5.1, BC, DC, CC and EC are shown to achieve peak improvement over no-side-channel one of 1.57, 1.51, 1.41 and 1.22, respectively. The percentage of optimal power allocated to the side channel is only a small portion of transmit power in the regime where the proposed schemes offer better performance.
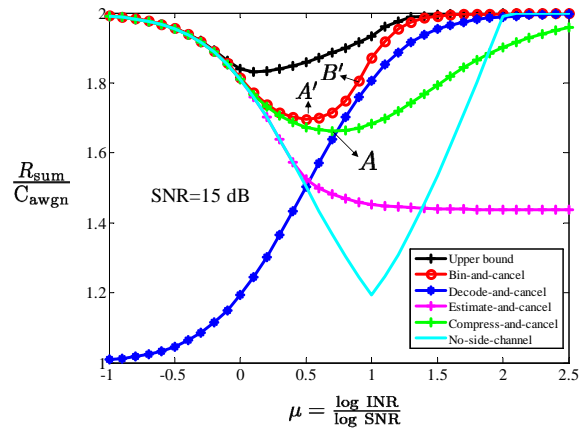
Figure 5.1: Multiplexing gain of proposed schemes versus no-side-channel achievable schemes for finite SNR when $W = 1$ and $\nu = \mu$.
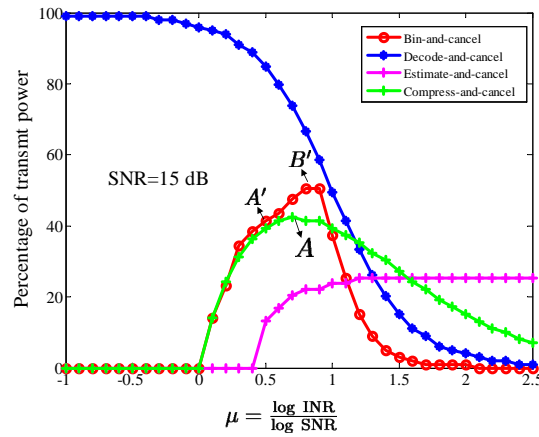
Figure 5.2: Optimal power allocated to the side channel which maximizes achievable sum-rates of proposed schemes for finite SNR when $W = 1$ and $\nu = \mu$

The explanation for the behavior of proposed schemes observed in Fig. 5.2 requires an understanding of the tradeoff for the power allocation between the side channel and main channel. The optimal power allocated to the side channel of both CC and BC schemes is a convex function of the interference channel gain according to Fig. 5.2. Specifically, for CC, when μ, the interference level, is low, as the interference level increases, more power needs to be allocated to the side channel to help cancel the interference and increase downlink rate R_1, which in turn decreases the uplink rate R_2. When moving to point A, as the interference level increases, both the interference channel gain and the side channel gain scale as $\nu = \mu$. The optimal power allocated to the side channel then declines, thus increasing the achievable sum-rate.

For BC, the achievable sum-rate can be expressed as

$$
\begin{aligned}
R_{\text{sum}}^{\text{BC}} \leq \max_{\substack{0 \leq \lambda \leq 1 \\ 0 \leq \beta \leq 1}} & C\left(\frac{\text{SNR}_1}{\beta \bar{\lambda} \text{INR} + 1}\right) + \min\Big\{C\left(\bar{\lambda}\text{SNR}_2\right), C\left(\beta\bar{\lambda}\text{SNR}_2\right) + \\
& C\left(\frac{\bar{\beta}\bar{\lambda}\text{INR}}{\text{SNR}_1 + \beta\bar{\lambda}\text{INR} + 1}\right) + WC\left(\frac{\lambda\text{SNR}_{\text{side}}}{W}\right)\Big\}.
\end{aligned}
\tag{5.2}
$$

The optimal β can be expressed as

$$
\beta^*(a) = \begin{cases}
\frac{(1+\bar{\lambda}\text{SNR}_2)(1+\text{SNR}_1)-a(1+\text{SNR}_1+\bar{\lambda}\text{INR})}{a\bar{\lambda}\text{SNR}_2(1+\text{SNR}_1+\bar{\lambda}\text{INR})-\bar{\lambda}\text{INR}(1+\bar{\lambda}\text{SNR}_2)} & \mu \leq 1 \\
0 & \mu \geq 1,
\end{cases}
\tag{5.3}
$$

where $a = \left(1 + \frac{\lambda\text{SNR}_{\text{side}}}{W}\right)^W$.

In the weak interference regime, from (5.3), we can find out that β^* is a non-increasing function of both μ and λ, implying that as INI becomes stronger, more information of M1 will be converted to common message. When INI is small, the optimal power allocated to the side channel (λ^*)rises as the interference level (μ) increases. Consequently, the interference from the private message of M1 at M2 is reduced as more information of M1 is converted into common message. However,

due to the increase of the amount of power allocated to the side channel, uplink rate R_2 suffers rate loss as less power is available for the main channel. After passing the point A', the increment of R_1 will surpass the decrement of R_2, resulting in an improvement of the sum-rate. At point B', β^* drops to zero, indicating that downlink is interference-free as no private message of M1 will interfere with M2. After reaching B', optimal power for the side channel decreases rapidly as the interference level (μ) increases in Fig. 5.2. Thus the uplink rate R_2 begin to rise. In the strong interference regime ($\mu \geq 1$), since all information of M1 is converted int common message, node M2 can decode all interference. However, the uplink rate R_2 is limited by the interference link. With the binning strategy through the side channel, we can also enhance R_2.

For DC, when $W=1$, the optimal percentage of power allocated to the side channel is

$$
\begin{aligned}
\lambda^*_{\mathrm{DC}} &= \arg \max_{\lambda}\ R^{\mathrm{DC}}_{\mathrm{sum}} \\
&= \frac{1}{1+\nu}.
\end{aligned}
$$

The corresponding maximized achievable sum-rate is

$$
R^{\mathrm{DC}}_{\mathrm{sum}}{}^* = \ C(\mathrm{SNR}) + C\left(\frac{\mathrm{SNR}_{\mathrm{side}}}{1+\nu}\right).
$$

When $\mu \to 0$, DC will have the worst performance. This is because when $\frac{\nu}{\mu}$ is fixed, the optimal power allocated to the side channel is inversely proportional to the interference level μ. Therefore, uplink node M1 needs to allocate most of its power to the side channel to decode the interfering signal in the very weak interference regime, with little power left to send its own data to the base station through the main channel. However, as the interference level increases, the optimal power allocated to the side channel drops rapidly, thus improving the performance of DC.

Comparing EC and DC, we can find out that EC performs better in the weak interference regimes while DC dominates in the strong interference regimes. The intuition behind this result is that when two mobile nodes are very close to each other which leads to strong INI, M2 can better decode the information from M1 by the side-channel. However, when the two mobile nodes are not so close resulting in weak INI, a statistical estimate of the interfering signal by the side-channel is better than decoding the signal to help cancel INI.

5.2 Asymptotic Multiplexing Gain

Assuming $\text{SNR} \gg 1, \text{INR} \gg 1$ and $\text{SNR}_{\text{side}} \gg W$, we compute the asymptotic multiplexing gain of our proposed schemes as $\text{SNR}, \text{SNR}_{\text{side}}, \text{INR} \to \infty$ and $\mu \geq 0, \nu \geq 0, W \geq 0$.

As $\text{SNR}, \text{SNR}_{\text{side}}, \text{INR} \to \infty$, in the weak interference regime (i.e., $0 \leq \mu < 1$), set the power for the private message of M1 at the level of Gaussian noise at the receiver of M2, namely, let $\beta = \frac{1}{\lambda \text{INR}}$. Thus for a fixed λ ($\lambda \neq 0$), we have

$$
\begin{aligned}
\frac{R_{\text{sum}}^{\text{BC}}}{C_{\text{single-user}}} &= \frac{W_m \min \left\{ \log\left(1 + \frac{\text{SNR}}{2}\right) + \log(1 + \bar{\lambda}\text{SNR}), \log\left(1 + \frac{\text{SNR} + \bar{\lambda}\text{INR} - 1}{2}\right) + \log\left(1 + \frac{\text{SNR}}{\text{INR}}\right) + W\log\left(1 + \lambda\frac{\text{SNR}_{\text{side}}}{W}\right) \right\}}{W_m \log(1 + \text{SNR})} \\
&\approx \frac{\min \left\{ 2\log(\text{SNR}), 2\log(\text{SNR}) - \log(\text{INR}) + W\log(\text{SNR}_{\text{side}}) \right\}}{\log(\text{SNR})} \\
&\approx \min\{2, 2 + W\nu - \mu\}.
\end{aligned}
$$
$$(5.4)$$

In the strong interference regime where $\mu \geq 1$, $\beta = 0$. As $\text{SNR}, \text{SNR}_{\text{side}}, \text{INR} \to \infty$, we have

$$
\begin{aligned}
\frac{R_{\text{sum}}^{\text{BC}}}{C_{\text{single-user}}} &\approx \frac{\min \left\{ 2\log(\text{SNR}), \log(\text{INR}) + W\log(\text{SNR}_{\text{side}}) \right\}}{\log(\text{SNR})} \\
&\approx \min\{2, \mu + W\nu\}.
\end{aligned}
$$
$$(5.5)$$

From Theorem 4, we have proved that the inner bound achieved by BC is within

one bit of the outer bound by a simple common-private power split when the power splitting of private message of M1 is set at the level of Gaussian noise at the receiver of M2, i.e., $\beta = \frac{1}{\lambda \text{INR}}$. Hence in the high SNR and INR limit, BC scheme is asymptotic optimal in that it is capacity-achieving for the Gaussian side-channel assisted three-node network. Therefore, the asymptotic multiplexing gain of the sum-capacity of Gaussian three-node full-duplex with side channel over signal-user capacity is

$$
\begin{aligned}
M^{\text{side-channel}} &= \frac{C_{\text{sum}}^{\text{side channel}}}{C_{\text{single-user}}} \\
&= M^{\text{BC}} = \begin{cases} \min\{2, 2 + W\nu - \mu\} & 0 \le \mu < 1 \\ \min\{2, \mu + W\nu\} & \mu \ge 1. \end{cases}
\end{aligned}
\tag{5.6}
$$

By comparing (5.6) to (2.27), we can derive the multiplexing gain improvement of side-channel sum-capacity over no-side-channel sum-capacity,

$$
\frac{M^{\text{side-channel}}}{M^{\text{No side-channel}}} = \begin{cases} \min\left\{\frac{2}{2-\mu}, 1 + \frac{W\nu}{2-\mu}\right\} & 0 \le \mu < 1 \\ \min\left\{\frac{2}{\mu}, 1 + \frac{W\nu}{\mu}\right\} & 1 \le \mu < 2. \end{cases}
\tag{5.7}
$$

When $W\nu = 0$, namely, there is no side channel available, (5.6) will degenerate into (2.27), and there is no improvement. From (5.7), we can see that the improvement depends on the interference level (i.e., μ), as well as the side channel condition (i.e., $W\nu$). In the weak interference regime where $\mu \in [0, 1)$, the improvement is an increasing function of the interference level, while in the strong interference regime where $\mu \ge 1$, the improvement will decrease as μ increases. Therefore, we can obtain the maximum multiplexing gain improvement when $\mu = 1$. The improvement rises as $W\nu$ increases till reaching the maximum multiplexing gain of 2. If $W\nu \ge 1$ and $\mu = 1$, then leveraging the side channel can double the asymptotic multiplexing gain.

Similarly, we can derive the asymptotic multiplexing of the suboptimal schemes,

$$M^{\mathrm{CC}} = \frac{R_{\mathrm{sum}}^{\mathrm{CC}}}{C_{\mathrm{single-user}}} = \begin{cases} \min\{2, 2 + W\nu - \mu\} & 0 \le \mu < 1 \\ \\ \min\{2, 1 + W\nu\} & \mu \ge 1, \end{cases} \qquad (5.8)$$

$$M^{\mathrm{DC}} = \frac{R_{\mathrm{sum}}^{\mathrm{DC}}}{C_{\mathrm{single-user}}} = \min\{2, 1 + W\nu\} \quad \mu \ge 0, \qquad (5.9)$$

$$M^{\mathrm{EC}} = \frac{R_{\mathrm{sum}}^{\mathrm{EC}}}{C_{\mathrm{single-user}}} = \begin{cases} \min\{2, 2 + \nu - \mu\} & 0 \le \mu < \nu + 1, W \in \mathbb{N}^+ \\ \\ 1 & \mu \ge \nu + 1, W \in \mathbb{N}^+. \end{cases} \qquad (5.10)$$

Comparing (5.6) and (5.8)-(5.10), we can find out that for all channel parameters and bandwidth ratio CC scheme is asymptotic sum-capacity achieving in the weak interference regime, while in the strong interference regime, the performance of CC agrees with DC scheme. The asymptotic multiplexing gain of CC is larger than that of DC and EC in the weak interference regime.

Now let us look at the effect of the side channel on the multiplexing gain of our proposed schemes. When $W = 1$, EC is also asymptotic sum-capacity achieving in the weak interference regime. Specifically, for EC scheme, when $W \ge 1$ and $\nu \ge \mu$, EC can achieve a asymptotic multiplexing gain of 2 for all interference level. And DC can achieve a asymptotic multiplexing gain of 2 for all interference level when $W\nu \ge 1$. When $W\nu \ge \mu$ for $\mu \in [0, 1)$, and $W\nu \ge 1$ for $\mu \ge 1$, BC and CC can achieve a asymptotic multiplexing gain of 2 for all interference level.

The asymptotic multiplexing gains of each scheme is plotted in Fig. 5.3. When $\nu < \mu$, the multiplexing gain of EC is a decreasing function of μ. This is because the side channel can not provide a better estimate of the interfering signal when the

side channel is worse than the interference link (i.e., main channel between M1 and M2). While for DC, when $\frac{\nu}{\mu}$ is fixed, the multiplexing gain of DC will scale with interference level. However, DC has poor performance when the interference level is very low.
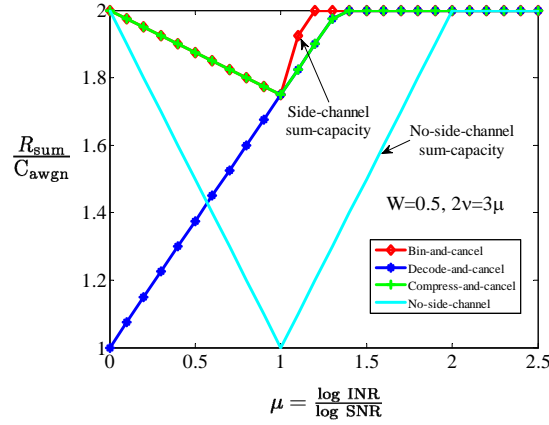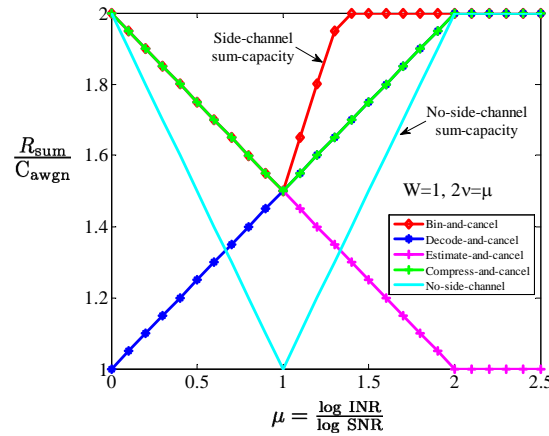

(a) $W < 1$ and $\nu \geq \mu$

(b) $W \geq 1$ and $\nu < \mu$

Figure 5.3: Asymptotic multiplexing gain for optimal scheme and suboptimal schemes versus no-side-channel sum-capacity. The suboptimal schemes are compress-and-cancel, decode-and-cancel and estimate-and-cancel.

5.3 Achievable Rate Region

Fig. 5.4 shows achievable rate regions of all proposed schemes by fixing channel parameters and bandwidth ratio. No-side-channel achievable region is encompassed by BC region, it is a special case of BC region when $W = 0$. Each of the suboptimal scheme has different achievable rate region. Specifically, for BC scheme, point Q corresponds to $\beta = 1$ when M1 sends all private message. This point coincides with the corner point of no-side-channel one when no power is allocated to the side channel. As β decreases, R_1 becomes larger owing to less interference. When moving to the point T which corresponds to $\beta = 0$, the downlink is not impaired by the interference any more as all information of M1 is converted to common message. By means of binning, the side channel will improve the common message rate of M1 that is restricted by the interference link of the main channel.
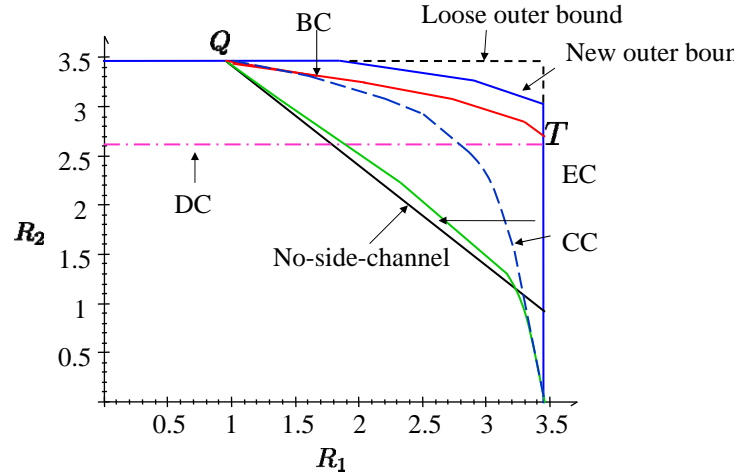

Figure 5.4: Achievable rate region of each proposed schemes versus no-side-channel achievable rate region when SNR=10 dB, $W = 1$ and $\nu = \mu = 1$.

5.4 Area gains

In order to have a better understanding of the performance of the simpler schemes for different distance regions of practical interest, we take the path loss model into consideration, and set the pathloss parameter as 3. We assume all transmitters have the same per-node power constraint, and the bandwidth ratio equals to 1.

We characterize the topological regimes where two simpler schemes DC and EC help leverage full-duplex gains. We consider an adaptive system that can choose between four schemes for managing inter-node interference: the two previous schemes when no side channel is utilized, treating interference as noise (TIN) and joint decoding (JD), and our proposed DC and EC schemes with optimal power allocation.

In Fig. 5.5(a), we show the percentage sum-rate gains of full-duplex over half-duplex counterpart for the adaptive system when transmit power is 0 dBm and noise floor is -100 dBm. We assume that the uplink mobile node M1 is fixed at a given distance from the BS, while the downlink mobile node M2 is located within a circular region of radius 200 meters from BS. The overall area gains of full-duplex by adopting the best scheme among the four range from 29.3% to 90.6%. In Table 5.1, we give the percentage rate improvement of each scheme.

Schemes	Avg. Rate Improvement over HD	Maximum	Minimum
JD and TIN	22.1%	90.6%	0.2%
Decode-and-cancel	49.4%	90.5%	23.8%
Estimate-and-cancel	19.8%	32%	-4.7%

Table 5.1: Rate improvement of each scheme over half-duplex counterpart.

Fig. 5.5(b) illustrates the area regions where each scheme offers the best performance among the four. The red color represents the area where JD scheme outperforms the other schemes. And the blue one represents the area where EC and TIN outperforms DC. The magenta color shows the areas where DC achieves more gains

than the rest of the three.

Under propagation model, we also compute the probability distribution of the usage of the side channel for improved interference cancellation. We assume the device-to-device side channel is not needed if the SINR of the interfered receiver is above a given capture threshold ξ which allows for successful transmission by satisfying a given bit/packet error probability. The probability when the side channel is not needed is given as

$$P_{\text{side not needed}} = \text{Prob}[\text{SINR} > \xi]. \tag{5.11}$$

Similarly, the probability of the usage of the side channel is defined if the SINR of the interfered receiver drops below a given threshold ξ and transmission is defined as failure. Hence the probability of the usage of side channel is:

$$
\begin{aligned}
P_{\text{side usage}} &= \text{Prob}[\text{SINR} \leq \xi] \\
&= 1 - \text{Prob}[\text{SINR} > \xi]. \tag{5.12}
\end{aligned}
$$

Taking into account both path loss due to distance and Rayleigh fading owing to multipath propagation. The received power from a mobile at distance d can be written as:

$$P_R = R^2 d^{-\eta} P_T, \tag{5.13}$$

where R is an independent and identically distributed (i.i.d.) random variable according to Rayleigh distribution with parameter σ, P_T is the transmission power and η is the pathloss parameter. The signal-to-interference-noise Ratio (SINR) at the receiver
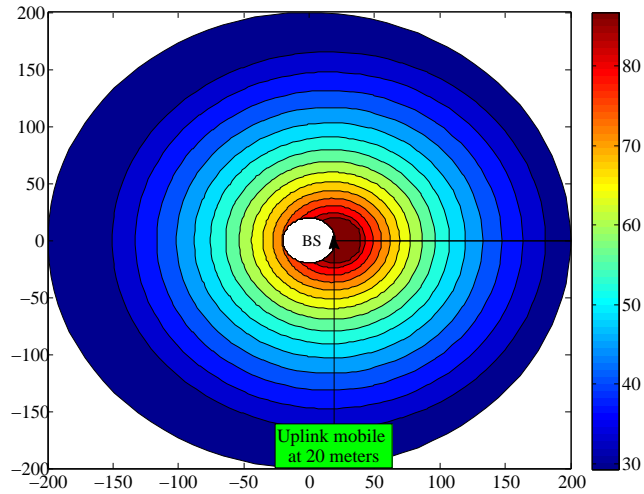
(a) The overall sum-rate gains (%) of full-duplex over the half-duplex counterpart by adopting different schemes which yield the maximum improvement.
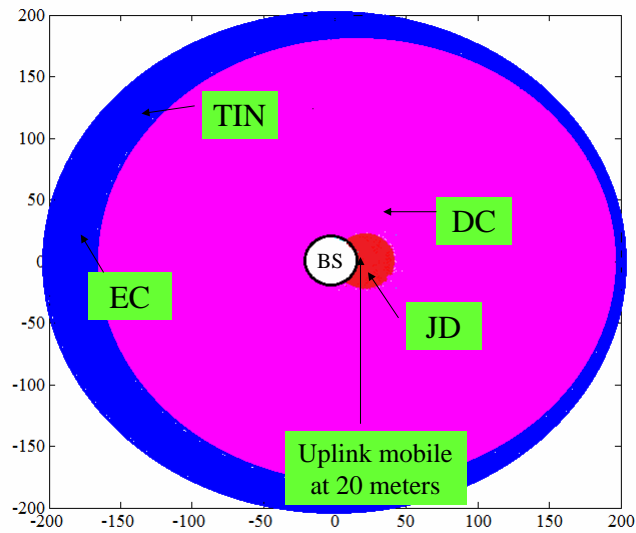
(b) Area region for different schemes

Figure 5.5: An adaptive system that can choose the best scheme to manage inter-node interference. Downlink mobile node M2 is located within a circular region of radius 200 meters from BS.

of M2 is defined as:

$$
\begin{aligned}
\text{SINR} &= \frac{P_{R_S}}{P_N + P_{R_I}} \\
&= \frac{R_S^2 d_S^{-\eta} P_S}{P_N + R_I^2 d_I^{-\eta} P_I} \\
&= \frac{R_S^2}{W + R_I^2 \frac{P_I}{P_S} \frac{\sigma_I^2}{\sigma_S^2} \left(\frac{d_I}{d_S}\right)^{-\eta}},
\end{aligned}
\tag{5.14}
$$

where P_N is the Gaussian noise with unit power, W is implicitly defined by (5.14). The subscript S denotes the intended receiver. Since $\frac{\sigma_I^2}{\sigma_S^2} = \frac{P_I}{P_S} \left(\frac{d_I}{d_S}\right)^{-\eta}$, hence we have

$$
\text{SINR} = \frac{R_S^2}{W + R_I^2 \left(\frac{P_I}{P_S} \left(\frac{d_I}{d_S}\right)^{-\eta}\right)^2}.
\tag{5.15}
$$

From (5.14), we have

$$
\begin{aligned}
P_{\text{side needed}} &= 1 - \text{Prob}[\text{SINR} > \xi] \\
&= 1 - \text{Prob}[P_{R_S} > \xi P_{R_I}] \\
&= 1 - \text{Prob}[R_S^2 > \xi R_I^2 \left(\frac{P_I}{P_S} \left(\frac{d_I}{d_S}\right)^{-\eta}\right)^2] \\
&= 1 - \int_0^\infty \frac{1}{2\sigma_I^2} e^{-\frac{x_I}{2\sigma_I^2}} \, dx_I \int_{\xi x_I \left(\frac{P_I}{P_S}\left(\frac{d_I}{d_S}\right)^{-\eta}\right)^2}^\infty \frac{1}{2\sigma_S^2} e^{-\frac{x_S}{2\sigma_S^2}} \, dx_S \\
&= \frac{\xi \left(\frac{P_I}{P_S} \left(\frac{d_I}{d_S}\right)^{-\eta}\right)^2}{1 + \xi \left(\frac{P_I}{P_S} \left(\frac{d_I}{d_S}\right)^{-\eta}\right)^2}.
\end{aligned}
\tag{5.16}
$$

We use practical link budget number to plot the probability of the usage of the side channel in Fig. 5.6, Fig. 5.7 and Fig. 5.8. And the link budget is listed in Table 5.2.

In Fig. 5.6, we can see that for higher data rate (larger capture threshold ξ) and larger transmit power ratio between mobile user and base station such as femtocell,

	Maximum	Minimum
Base station P_I	40 W	2 W
Mobile user P_S	2 W	1 W
Capture threshold ξ	20 dB (for high data rate)	0 dB (for low data rate)
Distance ratio $\frac{d_I}{d_S}$	2	0.1

Table 5.2: Link budget for propagation model with pathloss and rayleigh fading.

the probability of the usage of side channel is very high. And in Fig. 5.7 and Fig. 5.8, the probability of the usage of the side channel increases rapidly as the distance between the two mobile nodes and downlink decreases.
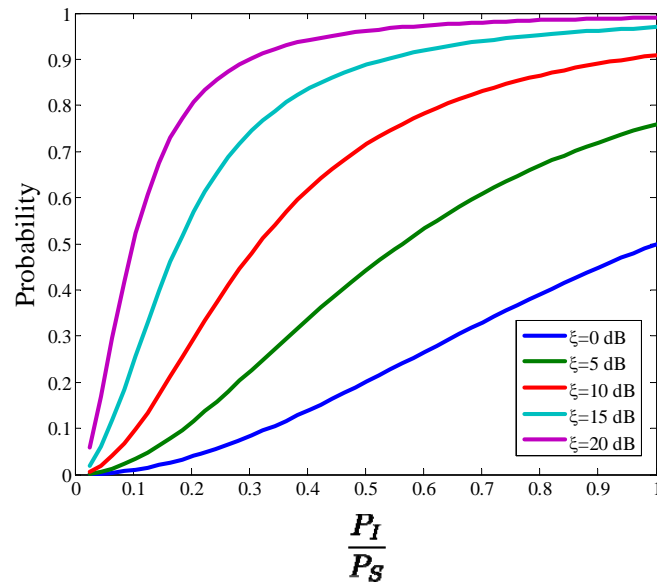

Figure 5.6: Probability of the usage of side channel versus transmit power ratio when the distance ratio $d_I/d_S = 1$.
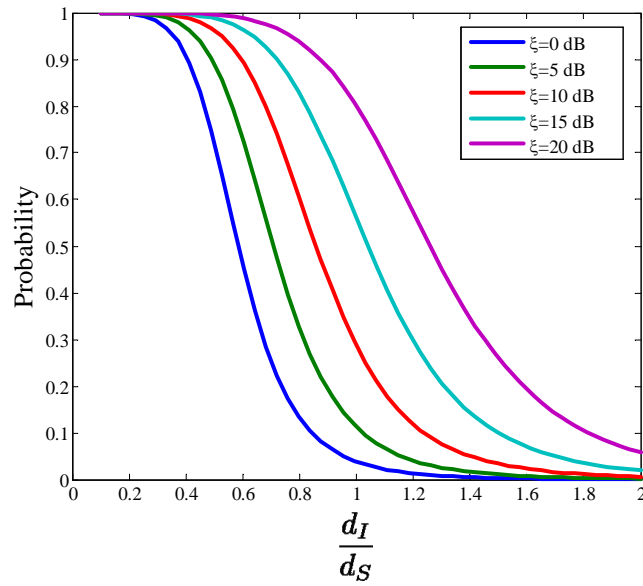
Figure 5.7: Probability of the usage of side channel versus distance ratio when the transmit power ration $P_I/P_S = 0.2$.
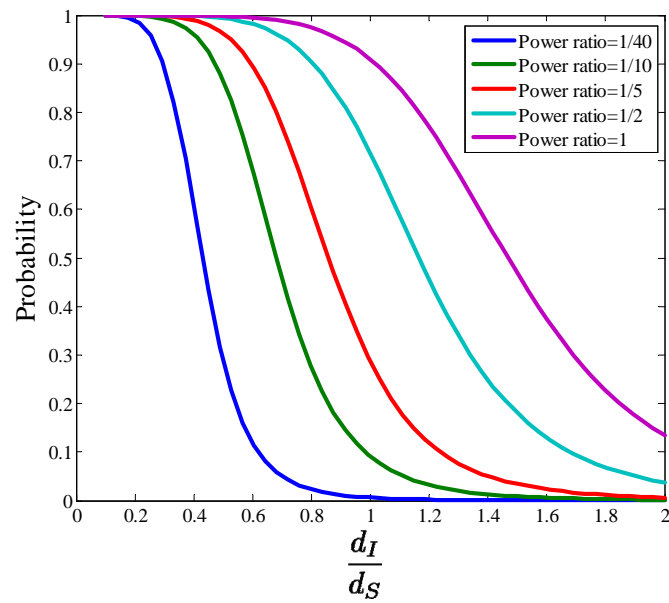

Figure 5.8: Probability of the usage of side channel versus distance ratio when capture threshold $\xi = 10$ dB.

Spectral Efficiency Discussion

The use of available side channel brings up an open question for spectral efficiency comparison between different systems. There are two systems for comparison in this thesis shown in Fig.6.1. The first one only uses the main channel in the three-node full-duplex network which is labeled as system 1, while the second one leverages the available side channel which is labeled as system 2.
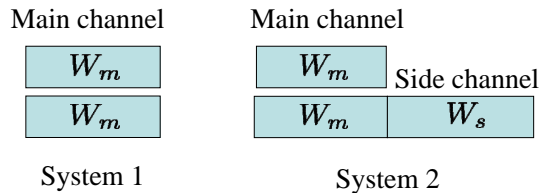

Figure 6.1: There are two systems for comparison with respect to spectral efficiency: one only uses the main channel, and the other one leverages the available side channel.

The spectral efficiency can be defined in two different ways, which is given as follows.

definition 1. Spectral efficiency (bits/s/Hz) is the ratio of achievable sum-rate and the total available bandwidth.

definition 2. spectral efficiency (bits/s/Hz) is the ratio of achievable sum-rate and the bandwidth that each system has used.

If the spectral efficiency (bits/s/Hz) is defined according to def. 1, then utilizing the available side channel will lead to higher spectral efficiency. However, if the spectral efficiency (bits/s/Hz) is defined according to def. 2, then for system 1,

$$\text{spectral efficiency}^1 \triangleq \frac{R_{\text{sum}}^{\text{No-side-channel}}}{W_m},$$

while for system 2,

$$\text{spectral efficiency}^2 \triangleq \frac{R_{\text{sum}}^{\text{side-channel}}}{W_m + W_s}.$$

In wideband power-limited regime, according to [20], we use spectral efficiency versus energy-per-information bit as the criterion to compare the spectral efficiency of these two systems. For simplicity, assuming the symmetric case where the transmit power of each sender is equal to P, and $\gamma_1 = \gamma_2 = 1$. Let E_b denote the transmitted energy per information bit, which can be Joules. When communication at sum-rate R_{sum} (bits/s), the following relationship is satisfied

$$\frac{E_b^i}{N_0} = \frac{2P}{N_0 R_{\text{sum}}^i}, i = 1, 2. \tag{6.1}$$

let x_i denote $\frac{E_b^i}{N_0}$ and y_i denote the spectral efficiency of each system. Thus for system 1, $y_1 = \frac{R_{\text{sum}}^1}{W_m}$ while for system 2, $y_2 = \frac{R_{\text{sum}}^2}{W_m + W_s}$. First we derive the relationship between x_1 and y_1,

$$y_1 = \begin{cases} \log\left(1 + \frac{x_1 y_1}{2 + \gamma_{21} x_1 y_1}\right) + \log\left(1 + \frac{x_1 y_1}{2}\right) & \gamma_{21} < 1 \\ \log\left(1 + \frac{(1 + \gamma_{21}) x_1 y_1}{2}\right) & 1 \le \gamma_{21} < 1 + \frac{x_1 y_1}{2} \\ 2\log\left(1 + \frac{x_1 y_1}{2}\right) & \gamma_{21} \ge 1 + \frac{x_1 y_1}{2}. \end{cases} \tag{6.2}$$

For system 2 when using the side channel, we can obtain y_2 as a function of x_2 by

BC scheme,

$$
y_2 =
\begin{cases}
\frac{1}{1+W}\log\left(1 + \frac{x_2 y_2}{2/(1+W)+\beta\bar{\lambda}\gamma_{21}x_2 y_2}\right) + \min\left\{\frac{1}{1+W}\log\left(1 + \frac{\bar{\lambda}(1+W)x_2 y_2}{2}\right),\right. \\[2mm]
\frac{1}{1+W}\log\left(1 + \frac{\beta\bar{\lambda}(1+W)x_2 y_2}{2}\right) + \frac{1}{1+W}\log\left(1 + \frac{\bar{\beta}\bar{\lambda}\gamma_{21}x_2 y_2}{2/(1+W)+\beta\bar{\lambda}\gamma_{21}x_2 y_2 + x_2 y_2}\right) \\[2mm]
\left. + \frac{W}{1+W}\log\left(1 + \frac{\lambda\gamma_3(1+W)x_2 y_2}{2W}\right)\right\}, & \gamma_{21} < 1 \\[4mm]
\frac{1}{1+W}\log\left(1 + \frac{(1+W)x_2 y_2}{2}\right) + \min\left\{\log\left(1 + \frac{\bar{\lambda}(1+W)x_2 y_2}{2}\right),\right. \\[2mm]
\left.\frac{1}{1+W}\log\left(1 + \frac{\bar{\lambda}\gamma_{21}x_2 y_2}{2/(1+W)+x_2 y_2}\right) + \frac{W}{1+W}\log\left(1 + \frac{\lambda\gamma_3(1+W)x_2 y_2}{2W}\right)\right\}. & \gamma_{21} \geq 1
\end{cases}
$$

(6.3)

From (6.3), we can find out that the spectral efficiency of system 2 achieved by BC scheme will improve as bandwidth ratio $W = \frac{W_s}{W_m}$ decreases. And increasing the ratio between γ_3 and γ_{21} will enhance the spectral efficiency of system 2. We can find a combination of small W and large γ_3 that allows system 2 to have higher spectral efficiency than system 1. Therefore for certain values of the two parameters of the side channel, i.e., W and γ_3, the resulting system 2 can not only yield higher achievable sum-rate, but also higher spectral efficiency.

As shown in Fig. 6.2, for certain channel parameters and bandwidth ratio, system 2 has higher spectral efficiency than system 1 with the same transmit energy per information bit. This implies that there exists some regimes of certain system parameters combination where leveraging the side channel can also lead to a higher spectral efficiency in addition to the achievable rate improvement.
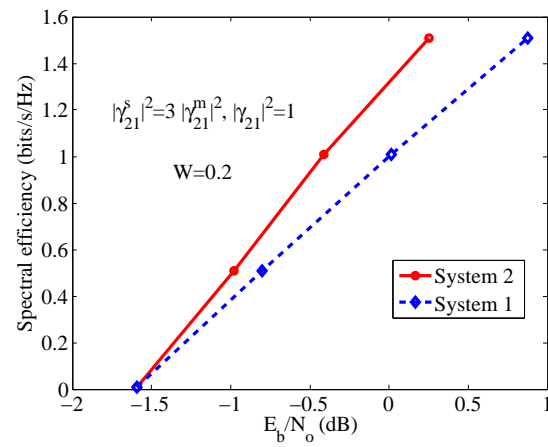
Figure 6.2: Spectral efficiencies of system 1 and system 2 when $W < 1, \gamma_3 > \gamma_{21} = 1$.

Conclusions

In a three-node full-duplex network where an infrastructure node communicates with half-duplex mobile nodes for both uplink and downlink simultaneously in the same band, one problem of paramount importance that needs to be resolved is the inter-node interference. We identify the availability of multi-radio interfaces on current mobile devices to create a side channel that allows for new approaches to mitigate inter-node interference. Therefore we propose distributed full-duplex architecture via wireless side channels for interference management.

In this thesis, we present four distributed full-duplex inter-node interference cancellation schemes by leveraging a device-to-device side channel for improved interference cancellation. We characterize the bounds on the capacity region of side-channel assisted three-node network and show that bin-and-cancel scheme can achieve within one bit of the capacity region for all values of channel parameters and is asymptotically optimal. The other three schemes are simpler but perform close to optimality only in certain regimes. Both analytical and numerical results demonstrate the factors that dominate the performance of the proposed schemes, which contributes to guiding the design of transceiver architecture.

References

[1] J. Bai and A. Sabharwal. Decode-and-cancel for interference cancellation in full-duplex networks. To appear: *46th Asilomar Conference on Signals, Systems and Computers*, nov 2012. 4, 1

[2] Y. Cao and B. Chen. Interference channel with one cognitive transmitter. In *Signals, Systems and Computers, 42nd Asilomar Conference on*, pages 1593 – 1597, oct 2008. 2.2

[3] A. Carleial. A case where interference does not reduce capacity (corresp.). *Information Theory, IEEE Transactions on*, 21(5):569 – 570, sep 1975. 2.2, 1

[4] S. Chen, M. Beach, and J. McGeehan. Division-free duplex for wireless applications. *Electronics Letters*, 34(2):147 –148, jan 1998. 1.1

[5] J. I. Choi, M. Jain, K. Srinivasan, P. Levis, and S. Katti. Achieving single channel, full duplex wireless communication. In *Proceedings of the sixteenth annual international conference on Mobile computing and networking*, MobiCom '10, pages 1–12, New York, NY, USA, 2010. ACM. 1.1

[6] M. Costa. Writing on dirty paper (corresp.). *IEEE Transactions on Information Theory*, 29(3):439–441, 1983. 2.3

[7] T. Cover and Y. Kim. Capacity of a class of deterministic relay channels. In *Information Theory, 2007. ISIT 2007. IEEE International Symposium on*, pages 591–595. IEEE, 2007. 3.1

[8] M. Duarte, C. Dick, and A. Sabharwal. Experiment-driven characterization of full-duplex wireless systems. *submitted to IEEE Transactions on Wireless Communication*, 2011. 1.1

[9] M. Duarte and A. Sabharwal. Full-duplex wireless communications using off-the-shelf radios: Feasibility and first results. In *Signals, Systems and Computers, 2010 Conference Record of the Forty Fourth Asilomar Conference on*, pages 1558 –1562, nov 2010. 1.1

[10] M. Duarte, A. Sabharwal, V. Aggarwal, R. Jana, K. Ramakrishnan, C. Rice, and N. Shankaranarayanan. Design and characterization of a full-duplex multi-antenna system for wifi networks. *submitted to IEEE Transactions on Vehicular Technology*, oct 2012. 1.1

[11] A. El Gamal and Y. Kim. *Network information theory*. Cambridge University Press, 2011. 2.3

[12] R. Etkin, D. Tse, and H. Wang. Gaussian interference channel capacity to within one bit. *Information Theory, IEEE Transactions on*, 54(12):5534 –5562, dec. 2008. 3.1

[13] E. Everett. Full-duplex infrastructure nodes: Achieving long-range with half-duplex mobiles. Master's thesis, Rice University, 2012. 1.1

[14] E. Everett, M. Duarte, C. Dick, and A. Sabharwal. Empowering full-duplex wireless communication by exploiting directional diversity. In *Proc. 2010 Asilomar Conference on Signals and Systems*, 2011. 1.1

[15] T. Han and K. Kobayashi. A new achievable rate region for the interference channel. *Information Theory, IEEE Transactions on*, 27(1):49–60, 1981. 2.2, 1

[16] B. Radunovic, D. Gunawardena, P. Key, A. Proutiere, N. Singh, V. Balan, and G. Dejean. Rethinking indoor wireless mesh design: Low power, low frequency, full-duplex. In *Wireless Mesh Networks (WIMESH 2010), 2010 Fifth IEEE Workshop on*. IEEE, 2010. 1.1

[17] A. Sahai, G. Patel, and A. Sabharwal. Pushing the limits of full-duplex: Design and real-time implementation, http://arxiv.org/abs/1107.0607. In *Rice University Technical Report TREE1104*, June 2011. 1.1

[18] I. Sason. On achievable rate regions for the gaussian interference channel. In *Information Theory, 2004. ISIT 2004. Proceedings. International Symposium on*, page 1, june-2 july 2004. 2.2, 1

[19] S. Seyedmehdi, J. Jiang, Y. Xin, and X. Wang. An improved achievable rate region for causal cognitive radio. In *Information Theory, 2009. ISIT 2009. IEEE International Symposium on*, pages 611–615. IEEE, 2009. 2.2

[20] S. Verdú. Spectral efficiency in the wideband regime. *Information Theory, IEEE Transactions on*, 48(6):1319–1343, 2002. 6

[21] A. Wyner and J. Ziv. The rate-distortion function for source coding with side information at the decoder. *IEEE Transactions on Information Theory*, 22(1):1–10, 1976. 3.2.1

[22] L. Zhou and W. Yu. Gaussian z-interference channel with a relay link: Achievability region and asymptotic sum capacity. *Information Theory, IEEE Transactions on*, 58(4):2413–2426, 2012. 3.1